Journal of Medicinal Chemistry

Article

Development of Dihydrodibenzooxepine Peroxisome Proliferator-Activated Receptor (PPAR) gamma Ligands of a Novel Binding Mode as Anticancer Agents: Effective Mimicry of Chiral Structures by Olefinic E/Z-Isomers

Keisuke Yamamoto, Tomohiro Tamura, Kazuki Henmi, Takeshi Kuboyama, Arata Yanagisawa, Masahiro Matsubara, Yuichi Takahashi, Michihiko Suzuki, Jun-ichi Saito, Kimihisa Ueno, and Satoshi Shuto

J. Med. Chem., **Just Accepted Manuscript** • DOI: 10.1021/acs.jmedchem.8b01200 • Publication Date (Web): 23 Oct 2018

ACS Publications

is published by the American Chemical Society. 1155 Sixteenth Street N.W., Washington, DC 20036

Development of Dihydrodibenzooxepine Peroxisome Proliferator-Activated Receptor (PPAR) gamma Ligands of a Novel Binding Mode as Anticancer Agents: Effective Mimicry of Chiral Structures by Olefinic *E/Z*-Isomers

Keisuke Yamamoto*[,†,‡], Tomohiro Tamura[†], Kazuki Henmi[†], Takeshi Kuboyama[†], Arata Yanagisawa[†], Masahiro Matsubara[†], Yuichi Takahashi[†], Michihiko Suzuki[†], Jun-ichi Saito[†], Kimihisa Ueno[†] and Satoshi Shuto*[,‡,§]

[†]Fuji Research Park, R&D Division, Kyowa Hakko Kirin, 1188, Shimotogari, Nagaizumi-cho, Sunto-gun, Shiuoka, Japan

[‡]Faculty of Pharmaceutical Sciences and [§]Center for Research and Education on Drug Discovery, Hokkaido University, Kita-12, Nishi-6, Kita-ku, Sapporo 060-0812, Japan

ABSTRACT : A novel class of PPARγ ligand **1** (EC_{50} = 197 nM) with a dibenzoazepin scaffold was identified through high-throughput screening campaign. To avoid the synthetically troublesome chiral center of **1**, its conformational analysis using the MacroModel was conducted, focusing on conformational flip of the tricyclic ring and the conformational restriction by the methyl group at the chiral center. Based on this analysis, scaffold hopping of dibenzoazepine into dibenzo[*b*,*e*]oxepine by replacing the chiral structures with the corresponding olefinic *E/Z* isomers was performed. Consequently, dibenzo[*b*,*e*]oxepine scaffold **9** was developed showing extremely potent PPARγ reporter activity (EC_{50} = 2.4 nM, efficacy = 9.5%) as well as differentiation-inducing activity against a gastric cancer cell line MKN-45 that was more potent than any other well-known PPARγ agonists in vitro (94% at 30 nM). The X-ray crystal structure analysis of **9** complexed with PPARγ showed that it had a unique binding mode to PPARγ ligand-binding domain that differed from that of any other PPARγ agonists identified thus far.

INTRODUCTION

Peroxisome proliferator-activated receptor gamma (PPARγ), a member of the nuclear receptor of the superfamily of ligand-inducible transcription factors, is known as a master regulator of adipose cells.[1,2] PPARγ is predominantly expressed in adipose tissue, while it is lower expressed in liver, muscle, and other tissue.[3] Owing to its outstanding insulin resistance-restoring activity, the thiozolidinedione (TZD) class of PPARγ full agonists, e.g., pioglitazone and rosiglitazone, have been used as antidiabetic drugs for the treatment of type 2 diabetes mellitus.[4,5,6]

There are three protein members of the PPAR family, PPARα, PPARγ and PPARβ/δ, each of which regulates different genes.[7] Many selective PPARγ agonists have been reported, and the structures of well-known PPARγ full agonists and ligands are shown in Figure 1.[8,9,10,11,12,13] PPARγ forms a heterodimer with retinoid X receptor (RXR) and the dimer binds to PPAR response element (PPRE).[14] Consequently regulating the expression of adipose-related genes that code adipocyte-related proteins, represented by adipocyte fatty acid-binding protein 2 (aP2),[15] adipose differentiation-related protein (ADFP) and adiponectin.[16] In this way, PPARγ agonists promote the differentiation of adipose tissues,[17] and there are many reports demonstrating that PPARγ agonists strongly promote the differentiation of fibroblast-like cells such as 3T3-L1 cells to adipocytes.[18,19,20,21]

Given the correlation between PPARγ activation and the differentiation of pre-adipocytes, PPARγ activation potentially induces the differentiation of cancer cells. Indeed, efatutazone (CS-7017), a potent PPARγ full agonist, showed differentiation-inducing activity in anaplastic thyroid carcinoma,[6,22] non-small cell lung cancer,[23] and pancreatic cancer[6] under low concentrations in vitro, while such differentiation effects have not been reported for any other PPARγ agonists. In addition, a recent phase 1 clinical study of efatutazone demonstrated that its treatment prolonged the overall survival of anaplastic carcinoma patients. However, several patients have reported adverse effects, such as localized edema, likely due to the chemical structure of the TZD moiety.[22,24]

Based on the abovementioned results, we suspected that it might be feasible to develop the novel therapeutic drugs for treating undifferentiated carcinoma with reduced side effects compared with efatutazone by creating

a novel PPARγ agonist with a scaffold other than TZD. We herein report our findings regarding a new class of PPARγ ligands of dihydrodibenzo[*b*,*e*]oxepine scaffold with very potent in vitro differentiation-inducing activity and a unique binding mode to the PPARγ ligand-binding domain (LBD), different from those of any known PPARγ agonists.

RESULT

Identification of Dihydrodibenzocycloheptene Derivative 5. PPARγ activation by efatutazone as observed in PPRE3-tk-Luc transfected DRO reporter gene assay is reportedly well correlated with the differentiation activity of cancer cell lines; for example, reporter gene assay found that the EC_{50} was approximately 1 nM, compared with 63% inhibition of cologenic growth at 1 nM.[9] We explored PPARγ agonists with a novel core structure for cancer therapy through a high-throughput screening campaign with PPARγ reporter gene assay using our chemical library. We ultimately identified dibenzoazepine derivative **1** as a hit, showing 24% efficacy of reporter gene expression at 1 μM compared with that of pioglitazone at 1 μM (100%); furthermore, this molecule had a scaffold that differed from any PPARγ agonists reported to date (Figure 2). The hit compound **1** was one of *R*/*S* enantiomers,[25] and one of the enantiomers was the eutomer. We believed that efficient lead optimization using a chiral compound as a lead might be troublesome, as the enantioselective construction of the asymmetric center adjacent to the nitrogen atom on the azepine ring was likely to require great effort. Therefore, to discover an alternative scaffold that was easy to prepare while mimicking the active form of **1**, a conformation analysis of each enantiomer of **1** was conducted.

The interaction between Tyr473 on PPARγ LBD and an acidic moiety of PPARγ full agonist is known to be essential for agonistic activity due to the stabilization of Helix12 that composes a section of the transcriptional coactivator binding region of the LBD.[26,27] This suggests that the acidic tetrazole in **1** may also be essential for the such activity. Then, we searched the dominant conformations focusing on the relative arrangement between the tetrazole group and the dibenzoazepine/dihydrodibenzocycloheptene moiety, using the molecular modeling tool MacroModel.

The conformations of 6/7/6-tricyclic ring systems like dibenzoazepine, which are often included in

pharmacologically active compounds, have been well studied (Figure 3).[28,29,30] These studies suggested that, in this kind of 6/7/6-tricyclic ring system, significant conformational change occurs with the reversal motion of the central seven-membered ring (conformational flip), as shown in Figure 3.

Figures 4 shows the structures of the tricyclic compounds (*R*)-**1'** and (*S*)-**1'** as model compounds for the conformational studies; these compounds had a simplified methyl substituent instead of imidazopyridine side chain at the 2-position of the dibenzoazepine moiety. The stable conformations of (*R*)-**1'** and its enantiomer (*S*)-**1'** calculated by MacroModel are shown in Figures 4A and 4B, respectively. The conformations were mainly changed depending on the flip of the central azepine ring (indicated with up and down based on the direction of 2-methyl group) and also the orientation of the tetrazole ring to the dibenzoazepine ring (indicated with *syn* and *anti* to the 2-methyl group). Thus, two significantly stable conformations *down-syn* and *up-anti* for (*R*)-**1'** and *up-syn* and *down-anti* for (*S*)-**1'** were obtained,[31] where the relationships between *down-syn* of (*R*)-**1'** and *up-syn* of (*S*)-**1'** and between *up-anti* of (*R*)-**1'**and *down-anti* of (*S*)-**1'** were enantiomeric of each other. These results show that the configurational difference, i.e. *R* or *S*, of the methyl-substituted asymmetric carbon center adjacent to the central 7-membered ring restricts the orientation of the tetrazole ring, probably due to the steric repulsion for the tricyclic ring structure, and accordingly one of the four conformationally restricted structures, *down-syn* and *up-anti* for (*R*)-**1'** and *up-syn* and *down-anti* for (*S*)-**1'**, might be a bioactive form binding to the LBD of PPARγ. This sort of effective conformational restriction depending on the configuration (*R* or *S*) of an asymmetric center due to the steric effect of a methyl or ethyl substituents attached to the asymmetric center has previously been reported by our laboratory.[32,33,34,35,36,37,38,39,40]

Given the results of the conformation analysis, we suspected that the *syn*/*anti*-orientation of the tetrazole moiety might be mimicked by the corresponding *E*/*Z*-olefinic structures without the asymmetric center. Stable conformations of designed olefinic model compounds **2'** and **3'** were calculated using MacroModel. As shown in Figures 4C and 4D, two stable conformations *down-Z* and *up-Z* for **2'** and *up-E* and *down-E* for **3'** were obtained depending on the flip of the dihydrocycloheptene ring, which likely mimicked the four structures: *down-syn* and *up-anti* for (*R*)-**1'** and *up-syn* and *down-anti* for (*S*)-**1'**, as we expected. These results showed that scaffold hopping of the asymmetric carbon substituent dibenzoazepine into dihydrodibenzocycloheptene might be feasible.

Figure 5 shows the superimposition of the most stable conformations of (*R*)-**1'** and (*S*)-**1'**, *E*/*Z* isomers **2'** and **3'**, respectively, in which the tricyclic ring and the tetrazole in four pairs (*down-syn* of (*R*)-**1'** vs. *down-Z* of **2'** (**5A**), *up-anti* of (*R*)-**1'** vs. *up-E* of **3'** (**5B**), *up-syn* of (*S*)-**1'** vs. *up-Z* of **2'** (**5C**), *down-anti* of (*S*)-**1'** vs. *dowm-E* of **3'** (**5D**)) were overlaid very closely. These results suggest that one of the stable conformer of dihydrodibenzocycloheptene derivatives **2** or **3** with the imidazopyridine side chain effectively mimic the bioactive conformer of the eutomer of **1**. We then synthesized *E*/*Z* isomers **2** and **3**, and another *E*/*Z* isomers **4** and **5**, which had an oxadiazolone instead of a tetrazole as an acidic moiety.

A reporter gene assay of the dihydrodibenzocycloheptene *E*/*Z*-isomers **2**-**5** at 1 μM was carried out, and the efficacies of the reporter gene expression relative to that of pioglitazone at 1 μM and EC_{50} values are summarized in Table 1. The *E*-isomers **2** and **4** were almost inactive; however, not only the efficacies of *Z*-isomers **3** and **5** were more than 20% at 1 μM, which was comparable to that of representative PPARγ ligands like INT-131 and metaglidasen (Table 3), but also their potencies were almost equal to that of hit compound **1** (197 nM vs. 251, 177 nM). This result suggested that the three-dimensional structure of the dihydrodibenzocycloheptene *Z*-isomers was likely to be analogous to that of the eutomer of **1**.

PPARγ ligands, such as INT-131 and metaglidasen, often show low efficacy (<20% of control) in HEK293 reporter gene assays; however, potent antidiabetic activities of these PPARγ ligands have been reported in preclinical and clinical studies.[10,41,42,43] In a preclinical study, the glucose level was significantly reduced by approximately 60% in INT-131 treated *db/db* diabetic model mice compared with vehicle mice, roughly equal to the effects of pioglitazone. Although the in vitro efficacies of **3** and **5** were analogous, we selected **5**[44] as the lead for further study due to its lower hydrophobicity than **3** (ClogP of **3** and **5**:5.76 vs. 6.03, calculated by ChemBioDraw Ultra 14.0).

Optimization of Lead Compound 5. To explore compounds having more potent differentiation activity than lead compound **5**, we performed the structural modification of **5**. The EC_{50} value in a PPARγ reporter gene assay was employed as an indicator of the activity, as the evaluation system was convenient and have been used effectively in previous developments of PPARγ ligands showing an excellent in vitro and in vivo antidiabetic activity.[45] Lead compound **5** had rather high lipophilicity (CLogP 6.03) and needed multistep

reactions for its synthesis due to the dihydrodibenzocycloheptene scaffold. To solve these issues, we designed and synthesized compound **6** (CLogP 5.00), in which the dihydrodibenzocycloheptene scaffold of **5** was replaced by an analogue tricyclic dibenzo[*b*,*e*]oxepine scaffold.

As a result, compound **6** with its novel dibenzo[*b*,*e*]oxepine scaffold had a good EC_{50} value of 84 nM, which was 2-fold more potent than the lead compound **5** and thereby encouraged us to prepare additional dibenzo[*b*,*e*]oxepine analogues. We further designed and synthesized benzoimidazole analogue **7**, removing the nitrogen atom on the imidazo[4,5-*b*]pyridine ring. Compound **7** showed promising activity (EC_{50} = 17 nM), that was approximately 10 times more potent than lead compound **5**.

Regarding modifications at the 2-position on the benzoimidazole moiety, we succeeded to find 2-propyl analogue **8**, which possessed the best in vitro activity in this chemical series, with an EC_{50} of 2.7 nM. Compound **9**, a 4-methyl analogue of **8**, was further synthesized and showed extremely potent *in vitro* activity with an EC_{50} of 2.4 nM comparable to that of **8**. This result suggested that modification at the 4-position of benzoimidazole was tolerated. To reduce the lipophilicity, analogues **10-13**, which had polar substituents at the 4-position, such as hydroxy and carbamoyl groups, were synthesized. Unfortunately, these compounds had lower efficacy and/or potency than **9**. Therefore, polar substituents at the 4-position were deemed unlikely to be tolerated. In addition, the imidazole analogues **14** and **15**, in which the benzoimidazole ring was replaced by a 4-aryllimidazole ring, also showed a significantly decreased activity compared with **9**.

Differentiation Effects of Dibenzo[*b*,*e*]oxepine Analogue 9 in Cancer Cells. We estimated the differentiation activity of dibenzo[*b*,*e*]oxepine derivative **9** as well as well-known PPARγ agonists using MKN-45 cells, a poorly differentiated gastric cancer cell line.[46] The differentiation activity was denoted by the aggregation effect, which was quantified by analyzing the morphological change using an IN Cell Analyzer.[47] As expected, **9** effectively induced the differentiation of MKN-45 cells at significantly lower concentrations (94% at 30 nM) than the other PPARγ full agonist and ligands, pioglitazone, INT-131, metaglidasen and FK-614, which showed EC_{50} values of >500 nM (Figure 6).

We next examined the effects of **9** on the gene expression (Figure 7). Quantitative polymerase chain reaction (qPCR) results of **9**-treated MKN-45 cells showed that it promoted the expressions of angiopoietin-like 4

(*angptl4*),[48] a PPARγ-regulated downstream gene and adipose differentiation-related protein (*adfp*)[49] at 100 nM, which was the concentration at which the effective induction of the MKN-45 cell aggregation by **9** was observed. In contrast, the expression of *vimentin*, a mesenchymal cell marker,[50] was effectively impaired at the same 100 nM concentration. Since the expression of these differentiation makers was changed at the same concentration range (10-100 nM), these data suggested that the differentiation activity of **9** was likely associated with transactivation activity on PPARγ.

As mentioned above, the differentiation-inducing activity of cancer cells was indicated by the aggregation activity of MKN-45 cells. We therefore plotted the EC_{50} values of compounds in a reporter gene assay with HEK293 versus those in the aggregation assay with MKN-45. As shown in Figure 8, the correlation between the EC_{50} values in the two different assay systems was extremely high (correlation coefficient $r^2 = 0.924$). These data suggest that **9** promotes the differentiation of MKN-45 cells due to its PPARγ agonistic activity.

Novel Binding Mode of 9 to PPARγ. A number of different crystal structures of the PPARγ LBD complexed with its ligands in various binding modes have been reported. The characteristic biological activity, particularly the remarkable differentiation against cancer cells, probably due to the unique scaffold of **9** as a PPARγ ligand prompted us to investigate its binding mode to PPARγ LBD. We successfully obtained the X-ray crystallographic structure of **9** binding to the PPARγ LBD (Figure 9A). The acidic proton of the oxadiazolone of **9** formed a hydrogen bond with the phenolic oxygen of Tyr473 on Helix12 (H12), which plays an important role in its agonistic activity.[51] The benzoimidazole side chain of **9** filled the region between Helix3 (H3) and Helix 5 (H5), known as the canonical ligand-binding pocket, with which interactions of a number of PPARγ ligands have been reported.[52] In contrast to the binding mode of rosiglitazone (Figure 9B), in the binding mode of **9**, Phe282 on H3, was moved toward H5 to form a small hydrophobic pocket where the rigid tricyclic structure was accommodated. In addition, one benzene ring of dibenzo[*b*,*e*]oxepine moiety of **9** occupied the hydrophobic region surrounded by H3 and helix 11 (H11), which was absent when complexed with rosiglitazone (Figure 9B). Furthermore, an edge-to-face interaction between the benzene ring of the benzoimidazole side chain and Phe282 was also observed.

Next, the binding mode of **9** was compared with those of other PPARγ ligands, including the recently reported MRL20 (Figure 1). Figure 9C shows the superimposed binding structures of PPARγ full agonist; rosiglitazone and PPARγ ligands; INT131, metaglidasen, MRL20,[52] and **9**. Although the acidic groups of rosiglitazone, MRL20 and **9** were closely overlaid and the benzoimidazole side chain of **9** filled the canonical ligand binding pocket like other ligands, the tricyclic dibenzo[*b*,*e*]oxepine moiety was accommodated in a hydrophobic pocket surrounded by H3 and H11, in contrast to all other ligands.

Finally, we confirmed the bioactive form. Among the four stable calculated conformations of (*R*)-**1** and (*S*)-**1** and the two stable conformations of **3**, *down-syn* of (*R*)-**1** and *down-Z* of **3** were well superimposable into the structure of **9** in the X-ray-analyzed binding mode (Figure 10). The acidic groups and the core structures of all compounds showed excellent overlap. These results demonstrated that the compound design based on a comparison of the global minimum energy conformations between each enantiomer of **1c** and **2c**, **3c** was effective. Given this good conformation overlap of **1** and **9**, we concluded that *(R)*-**1** is the eutomer and *down-syn* of (*R*)-**1** (aquamarine) and *down-Z* of **3** (bluepurple) are the bioactive form. The binding mode of **9** differed from those of any other PPARγ agonists reported to date. This characteristic binding mode of **9** might lead to a unique activity to PPARγ related to the differentiation effects.

Synthetic Chemistry. Compounds **2-11, 14** and **15** were prepared from *E*/*Z* congeners 2-(2-(hydroxymethyl)-10,11-dihydro-5*H*-dibenzocycloheptene-5-ylidene)propanenitrile **16*Z*** *and* **16*E***, and (*E*)-2-(8-(hydroxymethyl)dibenzo[*b*,*e*]oxepin-11(6*H*)-ylidene)propanenitrile **17*E*** (supporting information) respectively as summarized in Scheme 1. Mitsunobu reaction of **16*E*** and **16*Z*** with an imidazo[4,5-*b*]pyridine ring provided the corresponding coupling products **20*E***, **20*Z*** and **21*E*** respectively. Bromination or chlorination reaction of **17*E*** furnished halides **18** and **19**, respectively. The halides were reacted with azole rings to afford dibenzo[*b*,*e*]oxepine analogues **22*E*-29*E***.

The cyano groups of **20*E*** and **20*Z*** were cyclized by treatment with trimethylsilyl azide and then dibutyltin oxide gave tetrazoles **2** and **3**, respectively. Furthermore, the addition of hydroxyamine to the cyano group of **22*E*-24*E*** and **26*E*-29*E***, and subsequent acylation using ethyl chlorofomate, followed by treatment with *tert*-BuOK afforded the target oxadiazolone ring-closure compounds **4-11**, **14**, and **15**.

Conversion of the substituents at the 4-position of bennzo[*d*]imidazole ring of **25*E*,** was conducted as shown in Scheme 2. Hydrolysis of ester of **25*E***, followed by condensation with 2-aminoethanol gave **31**. Curtius rearrangement of 4-carboxylic acid in **30** and removal of the Boc group provided 4-sulfonamide **32**. Finally, the cyclization step was conducted as described above to give the target compounds **12** and **13**.

DISCUSSION and CONCLUSION

The conformation studies suggested that the *syn/anti*-orientation of the tetrazole moiety in the racemic dibenzoazepine of hit **1** would be mimicked by the corresponding *E/Z*-olefinic structures that did not contain an asymmetric center. Based on these findings, we designed a novel dihydrodibenzocycloheptene scaffold, and subsequent examination successfully led to the discovery of lead compound **5**, which possessed PPARγ reporter activity comparable to that of hit compound **1**. As a result of our lead optimization, dibenzo[*b*,*e*]oxepine derivative **9** with potent reporter and differentiation-inducing activities was obtained. The X-ray crystal structure of **9** complexed with PPARγ showed its unique binding mode to PPARγ LBD, which differed from those of any other PPARγ agonists identified to date. Interestingly, the calculated stable conformations of (*R*)-**1** (*down-syn*) overlapped well with the X-ray-analyzed LBD-binding structure of **9**, suggesting that (*R*)-**1** was the eutomer in which its bioactive form was the *down-syn* conformation.

In conclusion, we achieved scaffold hopping of hit compound **1** through a conformation study and successfully discovered a novel class of PPARγ ligand with potent cancer cell differentiation-inducing activity.

EXPERIMENTAL SECTION

General Methods. All reagents and solvents were procured from commercial sources and used as received. Thin layer chromatography (TLC) was carried out using Merck GmbH Precoated silica gel 60 F254. Chromatography on silica gel was carried out using prepacked silica gel cartridges (Yamazen Hi-Flash Column Silicagel or Wako Presep® Silicagel). Chemical shifts in ^{1}H NMR spectra were reported in δ values (ppm) relative to trimethylsilane. HPLC analyses were performed following conditions: Waters Xbrige® C18 column (3.5 μm, 4.6 mm × 50 mm), 30 °C column temperature, 1.0 mL/min flow rate, photodiode array detection (254 nm), and linear mobile phase gradient of 20%−90% B over 5 min, holding for 3.5 min at 20% B

(mobile phase A, 0.05% trifluoroacetic acid in water; mobile phase B, acetonitrile), by which the purities of final compounds were confirmed as >95%. Mass spectra were recorded on a Waters 2695 (ESI-MS).

(*E*)-3-((5-(1-(1*H*-tetrazol-5-yl)ethylidene)-10,11-dihydro-5*H*-dibenzo[*a*,*d*]cyclohepten-2-yl)methyl)-2-ethyl-5,7-dimethyl-3*H*-imidazo[4,5-*b*]pyridine (2). To a solution of **20*E*** (193 mg, 0.447 mmol) and dibutyltin oxide (44 mg, 0.18 mmol) in toluene (5.5 mL) was added trimethylsilylazide (0.474 mL, 3.57 mmol) and the solution was stirred at 80 °C for 48 h. To the reaction mixture was added methanol and the solution was concentrated to dryness. The obtained residue was then purified by flash column chromatography on silica gel (100:0 to 96:4 $CHCl_3$/methanol) to afford **2** (190 mg, 90%) as an amorphous. ^{1}H NMR (300 MHz, $CDCl_3$): δ 1.28 (t, J = 7.5 Hz, 3H), 2.31 (s, 3H), 2.53 (s, 3H), 2.58 (s, 3H), 2.66–2.78 (m, 4H), 3.09–3.25 (m, 2H), 5.41 (s, 2H), 6.88–6.91 (m, 2H), 6.99–7.02 (m, 2H), 7.13–7.32 (m, 4H). The proton of tetrazole was not observed. LC/MS (ESI, $[M + H]^+$, m/z) 476. HPLC: purity 99%, R_T 3.25 min.

(*Z*)-3-((5-(1-(1*H*-tetrazol-5-yl)ethylidene)-10,11-dihydro-5*H*-dibenzo[*a*,*d*]cyclohepten-2-yl)methyl)-2-ethyl-5,7-dimethyl-3*H*-imidazo[4,5-*b*]pyridine (3). A solution of **20*Z*** (212 mg, 0.49 mmol) in toluene (6.0 mL) at room temperature was treated with dibutyltin oxide (48 mg, 0.19 mmol) and trimethylsilylazide (0.516 mL, 3.88 mmol), and then the mixture was stirred at 80 °C for 48 h. To the reaction mixture was added methanol and the solution was concentrated to dryness. The obtained residue was then purified by flash column chromatography on silica gel (100:0 to 96:4 $CHCl_3$/methanol) to afford **3** (171 mg, 74%) as an amorphous. ^{1}H NMR (300 MHz, $CDCl_3$): δ 1.31 (t, J = 7.6 Hz, 3H), 2.33 (s, 3H), 2.54 (s, 3H), 2.61 (s, 3H), 2.68–2.82 (m, 2H), 2.75 (q, J = 7.6 Hz, 2H), 3.15–3.34 (m, 2H), 5.38 (s, 2H), 6.83–6.94 (m, 4H), 7.14–7.24 (m, 4H). The proton of tetrazole was not observed. LC/MS (ESI, $[M + H]^+$, m/z) 476. HPLC: purity 99%, R_T 3.57 min.

(*E*)-3-(1-(2-((2-ethyl-5,7-dimethyl-3*H*-imidazo[4,5-*b*]pyridin-3-yl)methyl)-10,11-dihydro-5*H*-dibenzo[*a*,*d*]cyclohepten-5-ylidene)ethyl)-1,2,4-oxadiazol-5(4*H*)-one (4). A solution of **20*E*** (192 mg, 0.44 mmol) in ethanol (4.4 mL) was treated with NH_2OH solution 50wt.% in water (0.54 mL, 8.9 mmol), and the resulting mixture was refluxed for 3 days. After the consumption of the starting material, the reaction mixture was poured into water and extracted twice with ethyl acetate. The combined organic layers were washed with brine, dried over sodium sulfate, and filtered. The organic layer was concentrated to dryness and the obtained

residue was dissolved in DMF (4.4 mL). To a stirred solution was added pyridine (44 μL, 0.53 mmol) and ethyl chloroformate (52 μL, 0.53 mmol) and the solution was stirred for 1h at room temperature. The reaction mixture was poured into saturated aqueous sodium bicarbonate solution and extracted twice with ethyl acetate. The combined organic layers were washed with brine, dried over sodium sulfate, and filtered. The organic layer was concentrated to give the residue. To a solution of the residue in toluene (4.4 mL) was added *tert*-BuOK (100 mg, 0.888 mmol) and the solution was stirred for 30 minutes at room temperature. The reaction mixture was poured into 5% aqueous citric acid solution and extracted twice with ethyl acetate. The combined organic layers were washed with brine, dried over sodium sulfate, and filtered. The organic layer was concentrated to give the residue. The obtained residue was then purified by flash column chromatography on silica gel (100:0 to 98:2 $CHCl_3$/methanol) to give **4** (166 mg, 76%) as an amorphous. ^{1}H NMR (300 MHz, $CDCl_3$): δ 1.31 (t, J = 7.5 Hz, 3H), 2.09 (s, 3H), 2.57 (s, 3H), 2.62 (s, 3H), 2.72–2.87 (m, 4H), 3.21–3.37 (m, 2H), 5.40 (s, 2H), 6.91–6.94 (m, 3H), 7.06–7.11 (m, 2H), 7.19–7.35 (m, 3H). The proton of oxadiazolone was not observed. LC/MS (ESI, $[M + H]^+$, m/z) 492. HPLC: purity 97%, R_T 3.63 min.

(*Z*)-3-(1-(2-((2-ethyl-5,7-dimethyl-3*H*-imidazo[4,5-*b*]pyridin-3-yl)methyl)-10,11-dihydro-5*H*-dibenzo[*a*,*d*]cyclohepten-5-ylidene)ethyl)-1,2,4-oxadiazol-5(4*H*)-one (5). To a stirred solution of **20*Z*** (197 mg, 0.456 mmol) in ethanol (4.5 mL) was added NH_2OH solution 50wt.% in water (0.56 mL, 9.24 mmol), and the solution was refluxed for 3 days. After the consumption of the starting material, the reaction mixture was poured into water and extracted twice with ethyl acetate. The combined organic layers were washed with brine, dried over sodium sulfate, and filtered. The organic layer was concentrated to dryness and the obtained residue was dissolved in DMF (4.5 mL). To a stirred solution was added pyridine (0.046 mL, 0.55 mmol) and ethyl chloroformate (0.054 mL, 0.55 mmol) and the solution was stirred for 1 h at room temperature. The reaction mixture was poured into saturated aqueous sodium bicarbonate solution and extracted twice with ethyl acetate. The combined organic layers were washed with brine, dried over sodium sulfate, and filtered. The organic layer was concentrated to give the residue. To a solution of the residue in toluene (4.5 mL) was added *tert*-BuOK (104 mg, 0.924 mmol) and the solution was stirred for 30 minutes at room temperature. The reaction mixture was poured into 5% aqueous citric acid solution and extracted twice with ethyl acetate. The combined organic layers were washed with brine, dried over sodium sulfate, and filtered. The organic layer

was concentrated to give the residue. The obtained residue was then purified by flash column chromatography on silica gel (100:0 to 98:2 $CHCl_3$/methanol) to give **5** (126 mg, 56%) as an amorphous. ^{1}H NMR (300 MHz, $CDCl_3$): δ 1.33 (t, J = 7.5 Hz, 3H), 2.11 (s, 3H), 2.55 (s, 3H), 2.63 (s, 3H), 2.75–2.83 (m, 2H), 2.79 (q, J = 7.5 Hz, 2H), 3.24–3.34 (m, 2H), 5.42 (s, 2H), 6.89–6.94 (m, 3H), 7.05–7.24 (m, 5H). The proton of oxadiazolone was not observed. LC/MS (ESI, $[M + H]^+$, m/z) 492. HPLC: purity 95%, R_T 3.85 min.

(*E*)-3-(1-(8-((2-ethyl-5,7-dimethyl-3*H*-imidazo[4,5-*b*]pyridin-3-yl)methyl)dibenzo[*b*,*e*]oxepin-11(6*H*)-ylidene)ethyl)-1,2,4-oxadiazol-5(4*H*)-one (6). To a stirred solution of **21*E*** (145 mg, 0.334 mmol) in ethanol (1.5 mL) was added NH_2OH solution 50wt.% in water (0.41 mL, 6.7 mmol), and the solution was refluxed for 3 days. After the consumption of the starting material, the reaction mixture was poured into water and extracted twice with ethyl acetate. The combined organic layers were washed with brine, dried over sodium sulfate, and filtered. The organic layer was concentrated to dryness and the obtained residue was dissolved in DMF (1.0 mL). To a stirred solution was added pyridine (0.053 mL, 0.66 mmol) and ethyl chloroformate (0.090 mL, 0.7 mmol) and the solution was stirred for 1h at room temperature. The reaction mixture was poured into saturated aqueous sodium bicarbonate solution and extracted twice with ethyl acetate. The combined organic layers were washed with brine, dried over sodium sulfate, and filtered. The organic layer was concentrated to give the residue. To a solution of the residue in toluene (3.0 mL) was added *tert*-BuOK (70 mg, 0.66 mmol) and the solution was stirred for 30 minutes at room temperature. The reaction mixture was poured into 5% aqueous citric acid solution and extracted twice with ethyl acetate. The combined organic layers were washed with brine, dried over sodium sulfate, and filtered. The organic layer was concentrated to give the residue. The obtained residue was then purified by flash column chromatography on silica gel (100:0 to 98:2 $CHCl_3$/methanol) to give **6** (60 mg, 36%) as an amorphous. ^{1}H-NMR (300 MHz, $CDCl_3$):δ 1.23 (t, J = 7.5 Hz, 3H), 2.06 (s, 3H), 2.54 (s, 3H), 2.58 (s, 3H), 2.68 (q, J = 7.5 Hz, 2H), 4.51 (d, J = 12.6 Hz, 1H), 5.28 (d, J = 12.6 Hz, 1H), 5.44 (s, 2H), 6.65 (dd, J = 8.3, 1.1 Hz, 1H), 6.80 (td, J = 7.5, 1.1 Hz, 1H), 6.90 (s, 1H), 7.01 (dd, J = 7.8, 1.7 Hz, 1H), 7.06 (s, 1H), 7.11–7.15 (m, 1H), 7.17 (br s, 2H). The proton of oxadiazolone was not observed. LC/MS (ESI, $[M + H]^+$, m/z) 494. HPLC: purity 99%, R_T 3.6 min.

(*E*)-3-(1-(8-((2-ethyl-1*H*-benzo[*d*]imidazol-1-yl)methyl)dibenzo[*b*,*e*]oxepin-11(6*H*)-ylidene)ethyl)-1,2,4-oxadiazol-5(4*H*)-one (7). To a stirred solution of **22*E*** (157 mg, 0.387 mmol) in ethanol (3.0 mL) was added

NH_2OH solution 50wt.% in water (0.712 mL, 11.6 mmol), and the solution was refluxed for 3 days. After the consumption of the starting material, the reaction mixture was poured into water and extracted twice with ethyl acetate. The combined organic layers were washed with brine, dried over sodium sulfate, and filtered. The organic layer was concentrated to dryness and the obtained residue was dissolved in THF (2.2 mL). To a stirred solution was added Et_3N (81 μL, 0.58 mmol) and ethyl chloroformate (56 μL, 0.58 mmol) and the solution was stirred for 1h at room temperature. The reaction mixture was poured into saturated aqueous sodium bicarbonate solution and extracted twice with ethyl acetate. The combined organic layers were washed with brine, dried over sodium sulfate, and filtered. The organic layer was concentrated to give the residue. To a solution of the residue in toluene (3.9 mL) was added *tert*-BuOK (65 mg, 0.58 mmol) and the solution was stirred for 30 minutes at room temperature. The reaction mixture was poured into 5% aqueous citric acid solution and extracted twice with ethyl acetate. The combined organic layers were washed with brine, dried over sodium sulfate, and filtered. The organic layer was concentrated to give the residue. The obtained residue was then purified by flash column chromatography on silica gel (99:1 to 95:5 $CHCl_3$/methanol) to to give **7** (8.7 mg, 4.8%) as an amorphous. ^{1}H-NMR (300 MHz, $CDCl_3$):δ 1.30 (t, J = 7.4 Hz, 3H), 2.31 (s, 3H), 2.90 (q, J = 7.4 Hz, 2H), 4.67 (d, J = 12.6 Hz, 1H), 5.29–5.44 (m, 2H), 5.53 (d, J = 12.6 Hz, 1H), 6.77–6.86 (m, 1H), 6.87–7.07 (m, 3H), 7.11–7.37 (m, 6H), 7.70–7.84 (m, 1H). The proton of oxadiazolone was not observed. LC/MS (ESI, $[M + H]^+$, m/z) 465. HPLC: purity 98%, R_T 3.45 min.

(*E*)-3-(1-(8-((2-propyl-1*H*-benzo[*d*]imidazol-1-yl)methyl)dibenzo[*b*,*e*]oxepin-11(6*H*)-ylidene)ethyl)-1,2,4-oxadiazol-5(4*H*)-one (8). To a stirred solution of **23*E*** (344 mg, 0.821 mmol) in ethanol (8.2 mL) was added NH_2OH solution 50wt.% in water (0.754 mL, 34.6 mmol), and the solution was refluxed for 3 days. After the consumption of the starting material, the reaction mixture was poured into water and extracted twice with ethyl acetate. The combined organic layers were washed with brine, dried over sodium sulfate, and filtered. The organic layer was concentrated to dryness and the obtained residue was dissolved in DMF (4.1 mL). To a stirred solution was added pyridine (80 μL, 0.98 mmol) and ethyl chloroformate (94 μL, 0.98 mmol) and the solution was stirred for 1h at room temperature. The reaction mixture was poured into saturated aqueous sodium bicarbonate solution and extracted twice with ethyl acetate. The combined organic layers were washed with brine, dried over sodium sulfate, and filtered. The organic layer was concentrated to give the residue. To a

solution of the residue in toluene (8.2 mL) was added *tert*-BuOK (138 mg, 1.23 mmol) and the solution was stirred for 30 minutes at room temperature. The reaction mixture was poured into 5% aqueous citric acid solution and extracted twice with ethyl acetate. The combined organic layers were washed with brine, dried over sodium sulfate, and filtered. The organic layer was concentrated to give the residue. The obtained residue was then purified by flash column chromatography on silica gel (100:0 to 99:1 $CHCl_3$/methanol) to give **8** (46 mg, 12%) as an amorphous. ^{1}H-NMR (300 MHz, $CDCl_3$):δ 0.94–1.06 (m, 3H), 1.80–1.96 (m, 2H), 2.28 (s, 3H), 2.74–2.84 (m, 2H), 4.71 (d, J = 12.6 Hz, 1H), 5.35 (s, 2H), 5.48 (d, J = 12.6 Hz, 1H), 6.74–6.86 (m, 1H), 6.86–6.97 (m, 1H), 6.98–7.04 (m, 1H), 7.04–7.32 (m, 7H), 7.64–7.78 (m, 1H). The proton of oxadiazolone was not observed. LC/MS (ESI, $[M + H]^+$, m/z) 479. HPLC: purity 99%, R_T 3.6 min.

(*E*)-3-(1-(8-((4-methyl-2-propyl-1*H*-benzo[*d*]imidazol-1-yl)methyl)dibenzo[*b*,*e*]oxepin-11(6*H*)-ylidene)ethyl)-1,2,4-oxadiazol-5(4*H*)-one (9). To a stirred solution of **24*E*** (449 mg, 1.04 mmol) in ethanol (10 mL) was added NH_2OH solution 50wt.% in water (1.9 mL, 31 mmol), and the solution was refluxed for 3 days. After the consumption of the starting material, the reaction mixture was poured into water and extracted twice with ethyl acetate. The combined organic layers were washed with brine, dried over sodium sulfate, and filtered. The organic layer was concentrated to dryness and the obtained residue was dissolved in DMF (5.2 mL). To a stirred solution was added pyridine (0.10 mL, 1.2 mmol) and ethyl chloroformate (0.12 mL, 1.2 mmol) the solution was stirred for 1h at room temperature. The reaction mixture was poured into saturated aqueous sodium bicarbonate solution and extracted twice with ethyl acetate. The combined organic layers were washed with brine, dried over sodium sulfate, and filtered. The organic layer was concentrated to give the residue. To a solution of the residue in toluene (10 mL) was added *tert*-BuOK (190 mg, 1.55 mmol) and the solution was stirred for 30 minutes at room temperature. The reaction mixture was poured into 5% aqueous citric acid solution and extracted twice with ethyl acetate. The combined organic layers were washed with brine, dried over sodium sulfate, and filtered. The organic layer was concentrated to give the residue. The obtained residue was then purified by flash column chromatography on silica gel (100:0 to 99:1 $CHCl_3$/methanol) to give **9** (109 mg, 22%) as an amorphous. ^{1}H-NMR (300 MHz, DMSO-d_6):δ 0.80–0.93 (m, 3H), 1.59–1.72 (m, 2H), 2.14 (s, 3H), 2.44–2.54 (m, 3H), 2.70–2.83 (m, 2H), 4.74–4.94 (m, 1H), 5.35–5.52

(m, 3H), 6.74–6.80 (m, 1H), 6.85–7.06 (m, 5H), 7.10–7.32 (m, 4H). The proton of oxadiazolone was not observed. LC/MS (ESI, $[M + H]^+$, m/z) 493. HPLC: purity 99%, R_T 3.7 min.

(*E*)-3-(1-(8-((4-(hydroxymethyl)-2-propyl-1*H*-benzo[*d*]imidazol-1-yl)methyl)dibenzo[*b*,*e*]oxepin-11(6*H*)-ylidene)ethyl)-1,2,4-oxadiazol-5(4*H*)-one (10). To a stirred solution of **26*E*** (90 mg, 0.20 mmol) in ethanol (2 mL) was added NH_2OH solution 50wt.% in water (0.368 mL, 6.00 mmol), and the solution was refluxed for 3 days. After the consumption of the starting material, the reaction mixture was poured into water and extracted twice with ethyl acetate. The combined organic layers were washed with brine, dried over sodium sulfate, and filtered. The organic layer was concentrated to dryness and the obtained residue was dissolved in THF (1 mL). To a stirred solution was added Et_3N (0.042 mL, 0.30 mmol) and ethyl chloroformate (0.029 mL, 0.30 mmol) the solution was stirred for 1h at room temperature. The reaction mixture was poured into saturated aqueous sodium bicarbonate solution and extracted twice with ethyl acetate. The combined organic layers were washed with brine, dried over sodium sulfate, and filtered. The organic layer was concentrated to give the residue. To a solution of the residue in toluene (2 mL) was added *tert*-BuOK (34 mg, 0.30 mmol) and the solution was stirred for 30 minutes at room temperature. The reaction mixture was poured into 5% aqueous citric acid solution and extracted twice with ethyl acetate. The combined organic layers were washed with brine, dried over sodium sulfate, and filtered. The organic layer was concentrated to give the residue. The obtained residue was then purified by flash column chromatography on silica gel (100:0 to 95:5 $CHCl_3$/methanol) to give **10** (10 mg, 10%) as an amorphous. ^{1}H-NMR (300 MHz, DMSO-d_6):δ 0.85-1.00 (m, 3H), 1.67–1.84 (m, 2H), 2.27 (s, 3H), 2.93–3.04 (m, 2H), 4.76 (d, J = 12.6 Hz, 1H), 5.06 (s, 2H), 5.41 (s, 2H), 5.56 (d, J = 12.6 Hz, 1H), 6.78–6.87 (m, 1H), 6.86–7.01 (m, 2H), 7.04–7.24 (m, 7H). The protons of oxadiazolone and OH were not observed. LC/MS (ESI, $[M + H]^+$, m/z) 509. HPLC: purity 98%, R_T 3.4 min.

(*E*)-3-(1-(8-((4-(2-hydroxypropan-2-yl)-2-propyl-1*H*-benzo[*d*]imidazol-1-yl)methyl)dibenzo[*b*,*e*]oxepin-11(6*H*)-ylidene)ethyl)-1,2,4-oxadiazol-5(4*H*)-one (11). To a stirred solution of **27*E*** (147 mg, 0.308 mmol) in ethanol (2 mL) was added NH_2OH solution 50wt.% in water (0.566 mL, 9.24 mmol), and the solution was refluxed for 3 days. After the consumption of the starting material, the reaction mixture was poured into water and extracted twice with ethyl acetate. The combined organic layers were washed with brine, dried over sodium sulfate, and filtered. The organic layer was concentrated to dryness and the obtained residue was

dissolved in THF (2 mL). To a stirred solution was added Et_3N (0.064 mL, 0.46 mmol) and ethyl chloroformate (0.044 mL, 0.46 mmol) the solution was stirred for 1 h at room temperature. The reaction mixture was poured into saturated aqueous sodium bicarbonate solution and extracted twice with ethyl acetate. The combined organic layers were washed with brine, dried over sodium sulfate, and filtered. The organic layer was concentrated to give the residue. To a solution of the residue in toluene (2 mL) was added *tert*-BuOK (52 mg, 0.46 mmol) and the solution was stirred for 30 minutes at room temperature. The reaction mixture was poured into 5% aqueous citric acid solution and extracted twice with ethyl acetate. The combined organic layers were washed with brine, dried over sodium sulfate, and filtered. The organic layer was concentrated to give the residue. The obtained residue was then purified by flash column chromatography on silica gel (100:0 to 95:5 $CHCl_3$/methanol) to give **11** (61 mg, 37%) as an amorphous. ^{1}H-NMR (300 MHz, DMSO-d_6):δ 0.92–1.06 (m, 3H), 1.71 (s, 6H), 1.78–1.98 (m, 2H), 2.31 (s, 3H), 2.70–2.82 (m, 2H), 4.77 (d, J = 12.6 Hz, 1H), 5.33 (s, 2H), 5.51 (d, J = 12.6 Hz, 1H), 6.70–6.87 (m, 1H), 6.87–6.98 (m, 1H), 6.98–7.24 (m, 8H). The protons of oxadiazolone and OH were not observed. LC/MS (ESI, $[M + H]^+$, m/z) 537. HPLC: purity 96%, R_T 3.7 min.

(*E*)-*N*-(2-hydroxyethyl)-1-((11-(1-(5-oxo-4,5-dihydro-1,2,4-oxadiazol-3-yl)ethylidene)-6,11-dihydrodibenzo[*b*,*e*]oxepin-8-yl)methyl)-2-propyl-1*H*-benzo[*d*]imidazole-4-carboxamide (12). To a stirred solution of **31** (240 mg, 0.474 mmol) in ethanol (2.4 mL) was added NH_2OH solution 50wt.% in water (0.73 mL, 24 mmol), and the solution was refluxed for 3 days. After the consumption of the starting material, the reaction mixture was poured into water and extracted twice with ethyl acetate. The combined organic layers were washed with brine, dried over sodium sulfate, and filtered. The organic layer was concentrated to dryness and the obtained residue was dissolved in CH_2Cl_2 (2.4 mL). To a stirred solution was added Et_3N (99 µL, 0.71 mmol) and ethyl chloroformate (68 µL, 0.71 mmol) the solution was stirred for 1 h at room temperature. The reaction mixture was poured into saturated aqueous sodium bicarbonate solution and extracted twice with ethyl acetate. The combined organic layers were washed with brine, dried over sodium sulfate, and filtered. The organic layer was concentrated to give the residue. To a solution of the residue in toluene (1.2 mL) was added *tert*-BuOK (106 mg, 0.948 mmol) and the solution was stirred for 30 minutes at room temperature. The reaction mixture was poured into 5% aqueous citric acid solution and extracted twice with ethyl acetate. The combined organic layers were washed with brine, dried over sodium sulfate, and filtered. The organic layer

was concentrated to give the residue. The obtained residue was then purified by flash column chromatography on silica gel (100:0 to 97:3 $CHCl_3$/methanol) to give **12** (70 mg, 26%) as an amorphous. ^{1}H-NMR (300 MHz, DMSO-d_6):δ 0.85–1.01 (m, 3H), 1.72–1.90 (m, 2H), 2.18 (s, 3H), 2.77–3.01 (m, 2H), 3.43–3.65 (m, 4H), 4.72–5.05 (m, 2H), 5.38–5.52 (m, 1H), 5.59 (s, 2H), 6.73–6.86 (m, 1H), 6.86–6.99 (m, 1H), 7.02–7.13 (m, 2H), 7.13–7.36 (m, 4H), 7.61–7.75 (m, 1H), 7.75–7.93 (m, 1H), 9.93–10.13 (m, 1H), 12.19 (br s, 1H). LC/MS (ESI, $[M + H]^+$, m/z) 566. HPLC: purity 99%, R_T 3.3 min.

(*E*)-*N*-(1-((11-(1-(5-oxo-4,5-dihydro-1,2,4-oxadiazol-3-yl)ethylidene)-6,11-dihydrodibenzo[*b*,*e*]oxepin-8-yl)methyl)-2-propyl-1*H*-benzo[*d*]imidazol-4-yl)methanesulfonamide (13). To a stirred solution of **32** (45 mg, 0.088 mmol) in ethanol (1.0 mL) was added NH_2OH solution 50wt.% in water (0.27 mL, 4.4 mmol), and the solution was refluxed for 3 days. After the consumption of the starting material, the reaction mixture was poured into water and extracted twice with ethyl acetate. The combined organic layers were washed with brine, dried over sodium sulfate, and filtered. The organic layer was concentrated to dryness and the obtained residue was dissolved in CH_2Cl_2 (1.0 mL). To a stirred solution was added Et_3N (18 μL, 0.13 mmol) and ethyl chloroformate (13 μL, 0.13 mmol) the solution was stirred for 1 h at room temperature. The reaction mixture was poured into saturated aqueous sodium bicarbonate solution and extracted twice with ethyl acetate. The combined organic layers were washed with brine, dried over sodium sulfate, and filtered. The organic layer was concentrated to give the residue. To a solution of the residue in toluene (1.0 mL) was added *tert*-BuOK (20 mg, 0.18 mmol) and the solution was stirred for 30 minutes at room temperature. The reaction mixture was poured into 5% aqueous citric acid solution and extracted twice with ethyl acetate. The combined organic layers were washed with brine, dried over sodium sulfate, and filtered. The organic layer was concentrated to give the residue. The obtained residue was then purified by flash column chromatography on silica gel (100:0 to 97:3 $CHCl_3$/methanol) to give **13** (14 mg, 28%) as an amorphous. ^{1}H-NMR (300 MHz, $CDCl_3$):δ 0.89–1.07 (m, 3H), 1.74–1.90 (m, 2H), 2.32 (s, 3H), 2.78–2.92 (m, 2H), 3.11 (s, 3H), 4.79 (d, J = 12.6 Hz, 1H), 5.38 (s, 2H), 5.55 (d, J = 12.6 Hz, 1H), 6.80–6.88 (m, 1H), 6.91–7.01 (m, 2H), 7.01–7.09 (m, 2H), 7.09–7.26 (m, 4H), 7.41–7.51 (m, 1H). The protons of oxadiazolone and sulfonamide were not observed. LC/MS (ESI, $[M + H]^+$, m/z) 572. HPLC: purity 99%, R_T 3.52 min.

(*E*)-3-(1-(8-((4-phenyl-2-propyl-1*H*-imidazol-1-yl)methyl)dibenzo[*b*,*e*]oxepin-11(6*H*)-ylidene)ethyl)-1,2,4-oxadiazol-5(4*H*)-one (14). To a stirred solution of **28*E*** (182 mg, 0.409 mmol) in ethanol (2.0 mL) was added NH_2OH solution 50wt.% in water (1.35 mL, 20.5 mmol), and the solution was refluxed for 3 days. After the consumption of the starting material, the reaction mixture was poured into water and extracted twice with ethyl acetate. The combined organic layers were washed with brine, dried over sodium sulfate, and filtered. The organic layer was concentrated to dryness and the obtained residue was dissolved in CH_2Cl_2 (2.0 mL). To a stirred solution was added Et_3N (86 μL, 0.62 mmol) and ethyl chloroformate (59 μL, 0.62 mmol), and the solution was stirred for 1 h at room temperature. The reaction mixture was poured into saturated aqueous sodium bicarbonate solution and extracted twice with ethyl acetate. The combined organic layers were washed with brine, dried over sodium sulfate, and filtered. The organic layer was concentrated to give the residue. To a solution of the residue in toluene (2.0 mL) was added *tert*-BuOK (91 mg, 0.82 mmol) and the solution was stirred for 30 minutes at room temperature. The reaction mixture was poured into 5% aqueous citric acid solution and extracted twice with ethyl acetate. The combined organic layers were washed with brine, dried over sodium sulfate, and filtered. The organic layer was concentrated to give the residue. The obtained residue was then purified by flash column chromatography on silica gel (100:0 to 90:10 $CHCl_3$/methanol) to give **14** (75 mg, 36%) as an amorphous. ^{1}H-NMR (300 MHz, $CDCl_3$):δ 0.92–1.02 (m, 3H), 1.67–1.87 (m, 2H), 2.26 (s, 3H), 2.58–2.69 (m, 2H), 4.78 (d, J = 12.6 Hz, 1H), 5.11 (s, 2H), 5.52 (d, J = 12.6 Hz, 1H), 6.81–6.87 (m, 1H), 6.87–6.95 (m, 1H), 6.98–7.11 (m, 4H), 7.11–7.27 (m, 3H), 7.27–7.39 (m, 2H), 7.68–7.79 (m, 2H). The proton of oxadiazolone was not observed. LC/MS (ESI, $[M + H]^+$, m/z) 505. HPLC: purity 95%, R_T 3.9 min.

(*E*)-3-(1-(8-((2-propyl-4-(pyridin-4-yl)-1*H*-imidazol-1-yl)methyl)dibenzo[*b*,*e*]oxepin-11(6*H*)-ylidene)ethyl)-1,2,4-oxadiazol-5(4*H*)-one (15). To a stirred solution of **29*E*** (43 mg, 0.097 mmol) in ethanol (1.0 mL) was added NH_2OH solution 50wt.% in water (0.32 mL, 4.8 mmol), and the solution was refluxed for 3 days. After the consumption of the starting material, the reaction mixture was poured into water and extracted twice with ethyl acetate. The combined organic layers were washed with brine, dried over sodium sulfate, and filtered. The organic layer was concentrated to dryness and the obtained residue was dissolved in CH_2Cl_2 (1.0 mL). To a stirred solution was added Et_3N (20 μL, 0.15 mmol) and ethyl chloroformate (14 μL, 0.15 mmol), and the solution was stirred for 1 h at room temperature. The reaction mixture was poured into

saturated aqueous sodium bicarbonate solution and extracted twice with ethyl acetate. The combined organic layers were washed with brine, dried over sodium sulfate, and filtered. The organic layer was concentrated to give the residue. To a solution of the residue in toluene (1.0 mL) was added *tert*-BuOK (22 mg, 0.19 mmol) and the solution was stirred for 30 minutes at room temperature. The reaction mixture was poured into 5% aqueous citric acid solution and extracted twice with ethyl acetate. The combined organic layers were washed with brine, dried over sodium sulfate, and filtered. The organic layer was concentrated to give the residue. The obtained residue was then purified by flash column chromatography on silica gel (100:0 to 90:10 $CHCl_3$/methanol) to give **15** (3.6 mg, 8.3%) as an amorphous. ^{1}H-NMR (300 MHz, $CDCl_3$):δ 0.93–1.04 (m, 3H), 1.67–1.85 (m, 2H), 2.32 (s, 3H), 2.55–2.71 (m, 2H), 4.67 (d, J = 12.6 Hz, 1H), 5.12 (s, 2H), 5.45 (d, J = 12.6 Hz, 1H), 6.79–6.89 (m, 2H), 6.89–7.02 (m, 1H), 7.07–7.32 (m, 5H), 7.55–7.68 (m, 2H), 8.32–8.45 (m, 2H). The proton of oxadiazolone was not observed. LC/MS (ESI, $[M + H]^+$, m/z) 506. HPLC: purity 96%, R_T 3.2 min.

(*E*)-2-(2-((2-ethyl-5,7-dimethyl-3*H*-imidazo[4,5-*b*]pyridin-3-yl)methyl)-10,11-dihydro-5*H*-dibenzo[*a*,*d*]cyclohepten-5-ylidene)propanenitrile (20*E*). To a stirred solution of **16*E*** (367 mg, 1.33 mmol), 2-ethyl-5,7-dimethyl-3*H*-imidazo[4,5-*b*]pyridine (367 mg, 2.09 mmol) and PPh_3 (1.4 g, 2.8 mmol, polymer-bound, ~approximately 3 mmol/g triphenylphosphine loading, Sigma-Aldrich) in THF (13 mL) was added di-*tert*-butyl azodicarboxylate (642 mg, 2.79 mmol), and the solution was stirred for 2 h at room temperature. The reaction mixture was filtered, and the filtrate was concentrated. The obtained residue was then purified by flash column chromatography on silica gel (80:20 to 65:35 hexane/ethyl acetate) to give **20*E*** (399 mg, 69%) as an amorphous. ^{1}H NMR (300 MHz, $CDCl_3$): δ 1.31 (t, J = 7.6 Hz, 3H), 1.99 (s, 3H), 2.58 (s, 3H), 2.63 (s, 3H), 2.73–2.88 (m, 2H), 2.76 (q, J = 7.6 Hz, 2H), 3.18–3.34 (m, 2H), 5.41 (s, 2H), 6.90–7.01 (m, 4H), 7.13 (dd, J = 7.1, 1.6 Hz, 1H), 7.18–7.28 (m, 2H), 7.39 (dd, J = 7.1, 1.6 Hz, 1H). LC/MS (ESI, $[M + H]^+$, m/z) 433.

(*Z*)-2-(2-((2-ethyl-5,7-dimethyl-3*H*-imidazo[4,5-*b*]pyridin-3-yl)methyl)-10,11-dihydro-5*H*-dibenzo[*a*,*d*]cyclohepten-5-ylidene)propanenitrile (20*Z*). To a stirred solution of **16*Z*** (399 mg, 1.45 mmol), 2-ethyl-5,7-dimethyl-3*H*-imidazo[4,5-*b*]pyridine (367 mg, 2.09 mmol) and PPh_3 (1.4 g, 2.8 mmol, polymer-bound, ~3 mmol/g triphenylphosphine loading, Sigma-Aldrich) in THF (13 mL) was added di-*tert*-butyl azodicarboxylate (642 mg, 2.79 mmol), and the solution was stirred for 2 h at room temperature. The reaction

mixture was filtered, and the filtrate was concentrated. The obtained residue was then purified by flash column chromatography on silica gel (80:20 to 65:35 hexane/ethyl acetate) to give **20*Z*** (376 mg, 68%) as an amorphous. ^{1}H NMR (300 MHz, $CDCl_3$): δ 1.31 (t, J = 7.4 Hz, 3H), 2.00 (s, 3H), 2.56 (s, 3H), 2.63 (s, 3H), 2.74–2.84 (m, 2H), 2.75 (q, J = 7.6 Hz, 2H), 3.20–3.30 (m, 2H), 5.40 (s, 2H), 6.83 (s, 1H), 6.88 (s, 1H), 6.97 (dd, J = 8.0, 1.6 Hz, 1H), 7.03–7.06 (m, 1H), 7.15–7.26 (m, 3H), 7.36 (d, J = 7.9 Hz, 1H). LC/MS (ESI, [M + H]$^+$, m/z) 433.

(*E*)-2-(8-((2-ethyl-5,7-dimethyl-3*H*-imidazo[4,5-*b*]pyridin-3-yl)methyl)dibenzo[*b*,*e*]oxepin-11(6*H*)-ylidene)propanenitrile (21*E*). 2-ethyl-5,7-dimethyl-3*H*-imidazo[4,5-*b*]pyridine (218 mg, 1.25 mmol) was added to a solution of **17*E*** (231 mg, 0.834 mmol), PPh_3 (1.4 g, 2.8 mmol, polymer-bound, ~approximately 3 mmol/g triphenylphosphine loading) and di-*tert*-butyl azodicarboxylate (382 mg, 1.66 mmol) in THF (4 mL), and the solution was stirred for 2 h at room temperature. The reaction mixture was filtered, and the filtrate was concentrated. The obtained residue was then purified by flash column chromatography on silica gel (70:30 to 20:80 hexane/ethyl acetate) to give **21*E*** (228 mg, 63%) as an amorphous. ^{1}H NMR (300 MHz, $CDCl_3$): δ 1.31 (t, J = 7.6 Hz, 3H), 2.24 (s, 3H), 2.58 (s, 3H), 2.65 (s, 3H), 2.77 (q, J = 7.6 Hz, 2H), 4.74 (d, J = 12.6 Hz, 1H), 5.40 (d, J = 12.6 Hz, 1H), 5.44–5.51 (m, 2H), 6.79–6.86 (m, 1H), 6.86–6.95 (m, 2H), 7.00–7.10 (m, 2H), 7.12–7.25 (m, 2H), 7.37–7.46 (m, 1H). LC/MS (ESI, [M + H]$^+$, m/z) 435.

(*E*)-2-(8-((2-ethyl-1*H*-benzo[*d*]imidazol-1-yl)methyl)dibenzo[*b*,*e*]oxepin-11(6*H*)-ylidene)propanenitrile (22*E*). 18 (300 mg, 1.01 mmol) was added to a solution of 2-ethyl-1*H*-benzo[*d*]imidazole (163 mg, 1.12 mmol) and K_2CO_3 (701 mg, 5.07 mmol) in DMF (5 mL), and the solution was stirred overnight at room temperature. The reaction mixture was poured into water and extracted twice with ethyl acetate. The combined organic layers were washed with brine, dried over sodium sulfate, and filtered. The organic layer was concentrated to give the residue. The obtained residue was then purified by flash column chromatography on silica gel (90:10 to 50:50 hexane/ethyl acetate) to give **22*E*** (318 mg, 77%) as an amorphous. ^{1}H NMR (300 MHz, $CDCl_3$): δ 1.43 (t, J = 7.6 Hz, 3H), 2.24 (s, 3H), 2.83 (q, J = 7.6 Hz, 2H), 4.72 (d, J = 12.6 Hz, 1H), 5.35 (s, 2H), 5.41 (d, J = 12.6 Hz, 1H), 6.80–6.99 (m, 3H), 7.02–7.15 (m, 2H), 7.16–7.33 (m, 4H), 7.43–7.50 (m, 1H), 7.72–7.83 (m, 1H). LC/MS (ESI, [M + H]$^+$, m/z) 406.

(*E*)-2-(8-((2-propyl-1*H*-benzo[*d*]imidazol-1-yl)methyl)dibenzo[*b*,*e*]oxepin-11(6*H*)-ylidene)propanenitrile (23*E*). 18 (300 mg, 1.01 mmol) was added to a solution of 2-propyl-1*H*-benzo[*d*]imidazole (179 mg, 1.12 mmol) and K_2CO_3 (701 mg, 5.07 mmol) in DMF (5 mL), and the solution was stirred overnight at room temperature. The reaction mixture was poured into water and extracted twice with ethyl acetate. The combined organic layers were washed with brine, dried over sodium sulfate, and filtered. The organic layer was concentrated to give the residue. The obtained residue was then purified by flash column chromatography on silica gel (90:10 to 70:30 hexane/ethyl acetate) to give **23*E*** (448 mg, 100%) as an amorphous. ^{1}H NMR (300 MHz, $CDCl_3$): δ 0.95–1.12 (m, 3H), 1.82–1.98 (m, 2H), 2.26 (s, 3H), 2.72–2.89 (m, 2H), 4.73 (d, J = 12.6 Hz, 1H), 5.35 (s, 2H), 5.41 (d, J = 12.6 Hz, 1H), 6.81–6.99 (m, 3H), 7.01–7.15 (m, 2H), 7.15–7.30 (m, 4H), 7.40–7.48 (m, 1H), 7.74–7.84 (m, 1H). LC/MS (ESI, $[M + H]^+$, m/z) 420.

(*E*)-2-(8-((4-methyl-2-propyl-1*H*-benzo[*d*]imidazol-1-yl)methyl)dibenzo[*b*,*e*]oxepin-11(6*H*)-ylidene)propanenitrile (24*E*). 19 (1.15 g, 3.61 mmol) was added to a solution of 4-methyl-2-propyl-1*H*-benzo[*d*]imidazole (691 mg, 3.97 mmol) and K_2CO_3 (2.49 g, 18.0 mmol) in DMF (20 mL), and the solution was stirred overnight at room temperature. The reaction mixture was poured into water and extracted twice with ethyl acetate. The combined organic layers were washed with brine, dried over sodium sulfate, and filtered. The organic layer was concentrated to give the residue. The obtained residue was then purified by flash column chromatography on silica gel (90:10 to 70:30 hexane/ethyl acetate) to give **24*E*** (891 mg, 57%) as an amorphous. ^{1}H NMR (300 MHz, $CDCl_3$): δ 0.95–1.05 (m, 3H), 1.74–1.91 (m, 2H), 2.25 (s, 3H), 2.69 (s, 3H), 2.78–2.88 (m, 2H), 4.73 (d, J = 12.6 Hz, 1H), 5.34 (s, 2H), 5.41 (d, J = 12.6 Hz, 1H), 6.80–6.98 (m, 3H), 6.98–7.18 (m, 5H), 7.17–7.28 (m, 1H), 7.38–7.48 (m, 1H). LC/MS (ESI, $[M + H]^+$, m/z) 434.

Methyl (*E*)-1-((11-(1-cyanoethylidene)-6,11-dihydrodibenzo[*b*,*e*]oxepin-8-yl)methyl)-2-propyl-1*H*-benzo[*d*]imidazole-4-carboxylate (25*E*). 19 (853 mg, 2.89 mmol) was added to a solution of methyl 2-propyl-1*H*-benzo[*d*]imidazole-4-carboxylate (600 mg, 2.75 mmol) and K_2CO_3 (1.9 g, 14 mmol) in DMF (16 mL), and the solution was stirred overnight at room temperature. The reaction mixture was poured into water and extracted twice with ethyl acetate. The combined organic layers were washed with brine, dried over sodium sulfate, and filtered. The organic layer was concentrated to give the residue. The obtained residue was then purified by flash column chromatography on silica gel (80:20 to 20:80 hexane/ethyl acetate) to give **25*E***

(970 mg, 74%) as an amorphous. ^{1}H NMR (300 MHz, $CDCl_3$): δ 0.97–1.10 (m, 3H), 1.83–1.97 (m, 2H), 2.24 (s, 3H), 2.84–2.99 (m, 2H), 4.04 (s, 3H), 4.64–4.75 (m, 1H), 5.28–5.49 (m, 3H), 6.82–6.96 (m, 3H), 7.02–7.14 (m, 2H), 7.18–7.30 (m, 2H), 7.31–7.39 (m, 1H), 7.39–7.46 (m, 1H), 7.89–8.00 (m, 1H). LC/MS (ESI, $[M + H]^+$, m/z) 478.

(*E*)-2-(8-((4-(hydroxymethyl)-2-propyl-1*H*-benzo[*d*]imidazol-1-yl)methyl)dibenzo[*b*,*e*]oxepin-11(6*H*)-ylidene)propanenitrile (26*E*). 19 (137 mg, 0.465 mmol) was added to a solution of (2-propyl-1*H*-benzo[*d*]imidazole-4-yl)methanol (97 mg, 0.51 mmol) and K_2CO_3 (321 mg, 2.33 mmol) in DMF (2.3 mL), and the solution was stirred overnight at room temperature. The reaction mixture was poured into water and extracted twice with ethyl acetate. The combined organic layers were washed with brine, dried over sodium sulfate, and filtered. The organic layer was concentrated to give the residue. The obtained residue was then purified by flash column chromatography on silica gel (50:50 to 20:80 hexane/ethyl acetate) to give **26*E*** (185 mg, 89%) as an amorphous. ^{1}H NMR (300 MHz, $CDCl_3$): δ 0.91–1.06 (m, 3H), 1.77–1.92 (m, 2H), 2.25 (s, 3H), 2.72–2.84 (m, 2H), 4.22–4.33 (m, 1H), 4.73 (d, J = 12.6 Hz, 1H), 5.09–5.19 (m, 2H), 5.35 (s, 2H), 5.41 (d, J = 12.6 Hz, 1H), 6.83–6.99 (m, 3H), 7.02–7.17 (m, 5H), 7.17–7.29 (m, 1H), 7.40–7.50 (m, 1H). LC/MS (ESI, $[M + H]^+$, m/z) 450.

(*E*)-2-(8-((4-(2-hydroxypropan-2-yl)-2-propyl-1*H*-benzo[*d*]imidazol-1-yl)methyl)dibenzo[*b*,*e*]oxepin-11(6*H*)-ylidene)propanenitrile (27*E*). A solution of K_2CO_3 (404 mg, 2.92 mmol) and 2-(2-propyl-1*H*-benzo[*d*]imidazol-4-yl)propan-2-ol (190 mg, 0.642 mmol) in DMF (3 mL) was treated with **19** (173 mg, 0.584 mmol), and the solution was stirred overnight at room temperature. The reaction mixture was poured into water and extracted twice with ethyl acetate. The combined organic layers were washed with brine, dried over sodium sulfate, and filtered. The organic layer was concentrated to give the residue. The obtained residue was then purified by flash column chromatography on silica gel (90:10 to 60:40 hexane/ethyl acetate) to give **27*E*** (295 mg, 100%) as an amorphous. ^{1}H NMR (300 MHz, $CDCl_3$): δ 0.89–1.07 (m, 3H), 1.73 (s, 6H), 1.78–1.98 (m, 2H), 2.25 (s, 3H), 2.70–2.85 (m, 2H), 4.75 (d, J = 12.6 Hz, 1H), 5.32 (s, 2H), 5.43 (d, J = 12.6 Hz, 1H), 6.76–7.01 (m, 4H), 7.01–7.34 (m, 5H), 7.39–7.51 (m, 1H). The proton of OH was not observed. LC/MS (ESI, $[M + H]^+$, m/z) 478.

(*E*)-2-(8-((4-phenyl-2-propyl-1*H*-imidazol-1-yl)methyl)dibenzo[*b*,*e*]oxepin-11(6*H*)-ylidene)propanenitrile (28*E*). To a stirred solution of **19** (131 mg, 0.445 mmol) and 4-phenyl-2-propyl-1*H*-imidazole (91 mg, 0.49 mmol) in DMF (2 mL) was added K_2CO_3 (307 mg, 2.22 mmol), and the solution was stirred overnight at room temperature. The reaction mixture was poured into water and extracted twice with ethyl acetate. The combined organic layers were washed with brine, dried over sodium sulfate, and filtered. The organic layer was concentrated to give the residue. The obtained residue was then purified by flash column chromatography on silica gel (100:0 to 70:30 hexane/ethyl acetate) to give **28*E*** (182 mg, 91%) as an amorphous. ^{1}H NMR (300 MHz, $CDCl_3$): δ 0.92–1.04 (m, 3H), 1.65–1.84 (m, 2H), 2.26 (s, 3H), 2.57–2.70 (m, 2H), 4.79 (d, J = 12.6 Hz, 1H), 5.11 (s, 2H), 5.43 (d, J = 12.6 Hz, 1H), 6.80–6.97 (m, 2H), 7.00–7.12 (m, 3H), 7.13–7.30 (m, 3H), 7.30–7.40 (m, 2H), 7.43–7.52 (m, 1H), 7.72–7.83 (m, 2H). LC/MS (ESI, $[M + H]^+$, m/z) 446.

(*E*)-2-(8-((2-propyl-4-(pyridin-4-yl)-1*H*-imidazol-1-yl)methyl)dibenzo[*b*,*e*]oxepin-11(6*H*)-ylidene)propanenitrile (29*E*). To a stirred solution of **19** (69 mg, 0.24 mmol) and 2-propyl-4-(pyridine-4-yl)-1*H*-imidazole (44 mg, 0.235 mmol) in DMF (1.5 mL) was added K_2CO_3 (160 mg, 1.18 mmol), and the solution was stirred overnight at room temperature. The reaction mixture was poured into water and extracted twice with ethyl acetate. The combined organic layers were washed with brine, dried over sodium sulfate, and filtered. The organic layer was concentrated to give the residue. The obtained residue was then purified by flash column chromatography on silica gel (100:0 to 90:10 $CHCl_3$/methanol) to give **29*E*** (43 mg, 40%) as an amorphous. ^{1}H NMR (300 MHz, $CDCl_3$): δ 0.93–1.06 (m, 3H), 1.68–1.85 (m, 2H), 2.25 (s, 3H), 2.61–2.73 (m, 2H), 4.81 (d, J = 12.6 Hz, 1H), 5.13 (s, 2H), 5.43 (d, J = 12.6 Hz, 1H), 6.79–6.97 (m, 2H), 7.03–7.32 (m, 4H), 7.35–7.55 (m, 2H), 7.57–7.67 (m, 2H), 8.47–8.60 (m, 2H). LC/MS (ESI, $[M + H]^+$, m/z) 447.

(*E*)-1-((11-(1-cyanoethylidene)-6,11-dihydrodibenzo[*b*,*e*]oxepin-8-yl)methyl)-2-propyl-1*H*-benzo[*d*]imidazole-4-carboxylic acid (30). To a stirred solution of **25*E*** (100 mg, 0.209 mmol) in ethanol (1 mL) was added 4M NaOH aqueous solution (1.0 mL, 4.0 mmol) and the solution was stirred for 2 h at 70 °C. The reaction mixture was acidified with 4 M HCl and the resultant solid was filtered, washed with water, and dried under reduced pressure to give **30** (86 mg, 89%) as a white solid.^{1}H NMR (300 MHz, DMSO-d_6): δ 0.87–1.01 (m, 3H), 1.60–1.82 (m, 2H), 2.18 (s, 3H), 2.96–3.12 (m, 2H), 4.93 (d, J = 12.6 Hz, 1H), 5.44 (d, J = 12.6 Hz, 1H), 5.76 (s, 2H), 6.80–6.87 (m, 1H), 6.90– 7.00 (m, 1H), 7.14–7.35 (m, 3H), 7.35–7.41 (m, 1H),

7.41–7.51 (m, 2H), 7.85–8.01 (m, 2H). The proton of CO_2H was not observed. LC/MS (ESI, $[M - H]^-$, m/z) 462.

(*E*)-*N*-(1-((11-(1-cyanoethylidene)-6,11-dihydrodibenzo[*b*,*e*]oxepin-8-yl)methyl)-2-propyl-1*H*-benzo[*d*]imidazol-4-yl)-3-hydroxypropanamide (31). To a stirred solution of **30** (220 mg, 0.475 mmol), EDCI·HCl (109 mg, 0.571 mmol) and HOBt·H_2O (87 mg, 0.57 mmol) in DMF (4 mL) was added 2-aminoethanol (57 μL, 0.95 mmol) and the solution was stirred overnight at room temparature. The reaction mixture was poured into saturated sodium hydrogen carbonae solution and the resultant solid was filtered, washed with water, and dried under reduced pressure. The obtained residue was then purified by flash column chromatography on silica gel (100:0 to 95:5 hexane/$CHCl_3$) to give **31** (241 mg, 99%) as an amorphous. ^{1}H NMR (300 MHz, $CDCl_3$): δ 0.88–1.13 (m, 3H), 1.79–1.97 (m, 2H), 2.26 (s, 3H), 2.72–2.88 (m, 2H), 3.38–3.59 (m, 1H), 3.71–3.86 (m, 2H), 3.86–3.97 (m, 2H), 4.68–4.78 (m, 1H), 5.33–5.49 (m, 3H), 6.81–6.96 (m, 3H), 7.03–7.15 (m, 2H), 7.20–7.37 (m, 3H), 7.41–7.50 (m, 1H), 8.03–8.17 (m, 1H), 10.22–10.35 (m, 1H). The protons of OH and amide were not observed. LC/MS (ESI, $[M + H]^+$, m/z) 507.

(*E*)-*N*-(1-((11-(1-cyanoethylidene)-6,11-dihydrodibenzo[*b*,*e*]oxepin-8-yl)methyl)-2-propyl-1*H*-benzo[*d*]imidazol-4-yl)methanesulfonamide (32). To a stirred solution of **30** (810 mg, 1.86 mmol) and Et_3N (1.3 ml, 9.3 mmol) in $CHCl_3$ (9 mL) was added DPPA (2.1 mL, 9.3 mmol) and the solution was stirred for 5 h at room temparature. *tert*-BuOH (9 ml) was added and the reaction mixture was stirred overnight at 100 °C. The reaction mixture was poured into saturated sodium hydrogen carbonate solution and extracted twice with $CHCl_3$. The combined organic layers were washed with brine, dried over sodium sulfate, and filtered. The organic layer was concentrated to give the residue. To a stirred solution of the obtained residue in CH_2Cl_2 (1 mL) was added TFA (0.31 mL) and the solution was stirred for 2 h at room temparature. The reaction mixture was poured into saturated sodium hydrogen carbonate solution and extracted twice with $CHCl_3$. The combined organic layers were washed with brine, dried over sodium sulfate, and filtered. The organic layer was concentrated to give the residue. The obtained residue was purified by flash column chromatography on silica gel (70:30 to 20:80 hexane/ethyl acetate). The resulting residue was dissolved in CH_2Cl_2 (2 mL) and DMAP (2 mg, 0.02 mmol) , $MeSO_2Cl$ (7.8 μL, 0.10 mmol) were added. The reaction mixture was stirred 5 h at room temparature. After the consumption of starting material, the mixture was poured into 2 mol/L HCl and

extracted twice with $CHCl_3$. The combined organic layers were washed with brine, dried over sodium sulfate, and filtered. The organic layer was concentrated to give the residue. The obtained residue was then purified by flash column chromatography on silica gel (80:20 to 20:80 hexane/ethyl acetate) to afford **32** (47 mg, 49%) as an amorphous. ^{1}H NMR (300 MHz, $CDCl_3$): δ 0.93–1.03 (m, 3H), 1.73–1.88 (m, 2H), 2.25 (s, 3H), 2.72–2.84 (m, 2H), 3.09 (s, 3H), 4.76 (d, J = 12.6 Hz, 1H), 5.33 (s, 2H), 5.43 (d, J = 12.6 Hz, 1H), 6.79–6.88 (m, 1H), 6.88–7.01 (m, 3H), 7.03–7.13 (m, 2H), 7.13–7.20 (m, 1H), 7.20–7.25 (m, 1H), 7.36–7.42 (m, 1H), 7.42–7.47 (m, 1H), 7.67–8.26 (m, 1H). LC/MS (ESI, $[M + H]^+$, m/z) 513.

Biological Methods.

Chimeric GAL4-PPARγ transactivation reporter assay. Test compounds were screened for agonist activity on PPARγ-GAL4 chimeric receptors in transiently transfected HEK293EBNA cells. The cells were maintained in Dulbecco's Modified Eagle Medium (DMEM; Thermo Fisher Scientific) containing 10% fetal bovine serum (Thermo Fisher Scientific), 100 U/mL penicillin, and 100 μg/ml streptomycin (Thermo Fisher Scientific) and incubated at 37 ^{o}C in 5% CO_2. To transfect the reporter constract into HEK293EBNA cells, cells were seeded at 1x 10^5 cells/ml in tissue culture dish (Iwaki, Chiba, Japan). After 24h incubation, transfections were performed with Superfect transfection reagent (QIAGEN) according to the instructions of the manufacturer. In brief, pM-human PPARγ/GAL4 expression vector and pZAC19-Luc vector were premixed and transfected into the cells followed by 2.5 h incubation. After a further 24 h incubation with growth medium, the transfected cells were seeded into 96-well assay plates, and test compounds were added (1-3000 nM, N = 3 per concentration). The test compounds were initially dissolved in DMSO, and then diluted in DMEM without any supplement. Steady-Glo luciferase assay reagent (Promega) was used as a substrate, and the luciferase activity was measured using the Microplate Scintillation and luminescence counter TopCount NXT (Packard, Groningen, Netherlands). The luciferase activity was normalized to that of pioglitazone at 1000 nM. The maximum activation (efficacy) of pioglitazone was taken as 100%. The efficacy of each compound was calculated as the percentage of the maximum activation obtained with pioglitazone. EC_{50} values were determined by the concentration that was 50% of its maximum activity using the XLFit.

MKN45 cell aggregation assay. MKN45 cells were aggregated when cells were incubated with PPARγ agonists. The cells were maintained in RPMI1640 medium (Thermo Fisher Scientific) containing 10% fetal bovine serum (Thermo Fisher Scientific), 100 U/mL penicillin, and 100 μg/ml streptomycin(Thermo Fisher Scientific) and incubated at 37 ^{o}C in 5% CO_2. Cells were seeded at 2500 cells/well in 96-well assay plates and incubated with test compounds, (1-1000 nM, N = 3 per concentration), for 5 days. Cell images were captured using an IN Cell Analyzer 1000 (GE healthcare). Nuclei were stained with the Hoechst 33342 (SIGMA) dyes, and the nuclei area was calculated. An area exceeding 1,015.58 μm^2 was defined as an aggregated cell cluster. The area ratio of aggregated cell clusters to the total cell area was calculated and taken as the formation rate of aggregation. The cell aggregation-inducing activity was normalized to that of **9**, with the maximum activity of **9** taken as 100%. The maximum activity of each compound was then calculated as the percentage of the maximum activity of **9**. EC_{50} values was determined as the concentration achieving 50% of its maximum activity using the XLFit.

MKN-45 cell gene expression analyses. MKN45 cells were seeded in assay plate and incubated with test compounds, (N = 3 per concentration), for 72 h. Total RNA was isolated from MKN45 cells using a RNeasy Mini Kit (QIAGEN). The cells were washed with cold PBS and lysed with buffer according to the instructions of the manufacturer. The RNA was reverse-transcribed using a SuperScript VILO cDNA Synthesis kit (Thermo Fisher Scientific) and synthesized to cDNA. Quantitative PCR was performed with Taqman fluorescent dye using an ABI PCR system. For PCR primers and probes, we used the Taqman® Gene Expression Assays system (Thermo Fisher Scientific) for ANGPTL4 (Hs_01101127_m1), VIM (Hs00958116_m1), and ADFP (Hs_00765634_m1). The PCR primer/probe sequences for GAPDH were as follows. Forward: ACAGTCAGCCGCATCTTCTTT, Reverse: CCCAATACGACCAAATCCGT, Probe: 6FAM-CGAGCCACATCGCTCAGACACCAT-Tamra (Operon). The gene expression value was corrected based on the value of GAPDH. The fold-induction ratio to the control was calculated.

Molecular modelling methods. The three-dimensional molecule structures of **1-3** were built using Schrödinger MacroModel10.9. The conformational search of each compound was performed using mixed torsional/low-mode sampling as implemented in MacroModel 10.9 with OPLS_2005 force field. The

conformational analysis was carried out without solvent. The default values were used for all other settings. The obtained global minimum energy conformations of the ligands were superimposed.

■ ASSOCIATED CONTENT

Supporting Information

General methods (S2)

Experimental details of tricyclic intermediates **16*E*/*Z***,**18**,**19** (S2)

NMR chart of compound **4** and **5** (S11)

Crystallographic data table of compound **9** (S13)

Electron density map of compound **9** (S14)

Molecular formula strings

Accession Codes

The X-ray structure of **9** with PPARγ LBD has been deposited with the Protein Data Bank. The code is 6AD9. We will release the atomic coordinates and experimental data upon article publication.

■ AUTHOR INFORMATION

Corresponding Authors

*For K.Y.: phone, +81-55-989-3989; fax, +81-55-986-7430; Email, keisuke.yamamoto@kyowa-kirin.co.jp; address, Small Molecule Drug Research Laboratories, Fuji Research Park, Shimotogari, Nagaizumi-cho, Sunto-gun, Shizuoka 411-8731, Japan.

*For S.S.: phone/fax, +81-11-706-3769; E-mail, shu@pharm.hokudai.ac.jp; address, Faculty of Pharmaceutical Sciences, Hokkaido University, Kita-12, Nishi-6, Kita-ku, Sapporo 060-0812, Japan.

Notes

The authors declare no competing financial interest.

■ ACKNOWLEDGMENTS

We thank Hiromi Nagai for supporting the synthesis of the tricyclic compounds. We thank Takahiro Kabeya for his assistance for the preparation of Figure 8. We thank Yusuke Yamada, Atsuko Sato and Mizuki Watanabe for the conformation study. We thank Kenta Nakajima for supporting our validation of the in vitro

assay data. We thank Hideyuki Onodera, Seiji Aratake and Kuniyuki Kishikawa for supporting the edit of this manuscript. We thank Daisuke Nakashima for screening the compounds for PAINS.

■ ABBREVIATIONS USED

DPPA, diphenylphosphoryl azide; DTBAD, di-*tert*-butyl azodicarboxylate; EDCI; 1-Ethyl-3-(3-dimethylaminopropyl)carbodiimide, HOBt, 1-hydroxybenzotriazole; PPRE, proliferator hormone response elements

ANCILLARY INFORMATION

Present author address

Kazuki Henmi, Arata Yanagisawa: Otemachi Financial City Grand Cube, 1-9-2 Otemachi, Chiyoda-ku, Tokyo, Japan

Masahiro Matsubara: Tokyo Research Park, 3-6-6 Asahi-machi, Machida-shi, Tokyo, Japan

RIFERENCES

(1) Tontonoz, P.; Hu, E.; Spiegelman, B. M. Stimulation of adipogenesis in fibroblasts by PPARγ2, a lipid-activated transcription factor. *Cell* **1994**, *79*, 1147–1156.

(2) Willson, T. M.; Lambert, M. H.; Kliewer, S. A. Peroxisome proliferator-activated receptor gamma and metabolic disease. *Annu. Rev. Biochem.* **2001**, *70*, 341–367.

(3) Evans, R. M.; Barish, G. D; Wang, Y. X. PPARs and the complex journey to obesity. *Nat. Med.* **2004**, *10*, 355–361.

(4) Parulkar, A. A.; Pendergrass, M. L.; Granda-Ayala, R.; Lee, T. R.; Fonseca, V. A. Nonhypoglycemic effects of thiazolidinediones. *Ann. Intern. Med*. **2001**, *134*, 61–71.

(5) Lehmann, J. M.; Moore, L. B.; Smith-Oliver, T. A.; Wilkison, W. O.; Willson, T. M.; Kliewer, S. A. An antidiabetic thiazolidinedione is a high affinity ligand for peroxisome proliferator-activated receptor γ (PPARγ). *J. Biol. Chem.* **1995**, *270*, 12953–12956.

(6) Forman, B. M.; Tontonoz, P.; Chen, J.; Brun, R. P.; Spiegelman, B. M.; Evans, R. M. 15-deoxy-$\Delta^{12,14}$-prostaglandin J_2 is a ligand for the adipocyte determination factor PPARγ. *Cell* **1995**, *83*, 803–812.

(7) Barish, G.D.; Narkar, V.A.; Evans R.M. PPARδ: a dagger in the heart of the metabolic syndrome. *J. Clin. Invest.* **2006**, *116*, 590–597.

(8) Shimazaki, N.; Togashi, N.; Hanai, M.; Isoyama, T.; Wada, K.; Fujita, T.; Fujiwara, K.; Kurakata, S. Anti-tumour activity of CS-7017, a selective peroxisome proliferator-activated receptor gamma agonist of thiazolidinedione class, in human tumour xenografts and a syngeneic tumour implant model. *Eur. J. Cancer* **2008**, *44*, 1734–1743.

(9) Copland, J. A.; LA Marlow, L. A.; Kurakata, S; Fujiwara, K; Wong, A. K. C.; Kreinest, P. A.; Williams, S. F.; Haugen, B. R.; Klopper, J. P.; Smallridge, R. C. Novel high-affinity PPARγ agonist alone and in combination with paclitaxel inhibits human anaplastic thyroid carcinoma tumor growth via $p21^{WAF1/CIP1}$. *Oncogene* **2006**, *25*, 2304–2317.

(10) Motani, A.; Wang, Z.; Weiszmann, J.; McGee, L. R.; Lee, G.; Liu, Q.; Staunton, J.; Fang, Z.; Fuentes, H.; Lindstrom, M.; Liu, J.; Biermann, D. H.; Jaen, J.; Walker, N. P.; Learned, R. M.; Chen, J. L.; Li, Y. INT131: a selective modulator of PPAR gamma. *J. Mol. Biol.* **2009**, *386*, 1301−1311.

(11) Gregoire, F. M.; Zhang, F.; Clarke, H. J.; Gustafson, T. A.; Sears, D. D.; Favelyukis, S.; Lenhard, J.; Rentzeperis, D.; Clemens, L. E.; Mu, Y.; Lavan, B. E. MBX-102/JNJ39659100, a novel peroxisome proliferator-activated receptor-ligand with weak transactivation activity retains antidiabetic properties in the absence of weight gain and edema. *Mol. Endocrinol* **2009**, *23*, 975–988.

(12) Minoura, H.; Takeshita, S.; Yamamoto, T.; Mabuchi, M.; Hirosumi, J.; Takakura, S.; Kawamura, I.; Seki, J.; Manda, T.; Ita, M.; Mutoh, S. Ameliorating effect of FK614, a novel nonthiazolidinedione peroxisome proliferator-activated receptorγ agonist, on insulin resistance in Zucker fatty rat. *Eur. J. Pharm.* **2005**, *519*, 182–190.

(13) Spiegelman's group most recently described that low efficacy PPARgamma agonists inhibited phosphorylation of ser273 of PPARgamma. Khandekar, M. J.; Banks, A. S.; Laznik-Bogoslavski, D.; White, J. P.; Choi, J. H.; Kazak, L.; Lo, J. C.; Cohen, P.; Wong, K.-K.; Kamenecka, T. M.; Griffin, P. R.; Spiegelman,

B. M. Noncanonical agonist PPARγ ligands modulate the response to DNA damage and sensitize cancer cells to cytotoxic chemotherapy. *Proc. Natl. Acad. Sci. U.S.A.* **2018**, *115*, 561–566.

(14) Lehrke, M., Lazar, M.A. The many faces of PPARgamma. *Cell* **2005**, *123*, 993–999.

(15) Medina-Gomez, G.; Gray, S.; Vidal-Puig, A. Adipogenesis and lipotoxicity: role of peroxisome proliferator-activated receptor gamma (PPARgamma) and PPARgamma coactivator-1 (PGC1). *Public Health Nutr*. **2007**, *10*, 1132–1137.

(16) Iwaki, M.; Matsuda, M.; Maeda, N.; Funahashi, T.; Matsuzawa, Y.; Makishima, M.; Shimomura, I. Induction of adiponectin, a fat-derived antidiabetic and antiatherogenic factor, by nuclear receptors. *Diabetes* **2003**, *52*, 1655–1663.

(17) Barak, Y.; Nelson, M. C.; Ong, E. S.; Jones, Y. Z.; Ruiz-Lozano, P.; Chien, K. R.; Koder, A.; Evans, R. M. PPARγ is required for placental, cardiac, and adipose tissue development. *Mol. Cell* **1999**, *4*, 585–595.

(18) Lehmann, J. M.; Moore, L. B.; Smith-Oliver, T. A.; Wilkinson, W. O.; Willson, T. M.; Kliewer, S. A. An antidiabetic thiazolidinedione is a high affinity ligand for peroxisome proliferator-activated receptor γ (PPARγ). *J. Biol. Chem.* **1995**, *270,* 12953–12956.

(19) Kliewer, S. A.; Lenhard, J. M.; Willson, T. M.; Patel, I.; Morris, D. C.; Lehmann, J. M. A Prostaglandin J2 metabolite binds peroxisome proliferator-activated receptor γ and promotes adipocyte differentiation. *Cell*, **1995**, *83*, 813–819.

(20) Fukui, Y.; Masui, S.; Osada, S.; Umesono, K.; Motojima, K. A new thiazolidinedione, NC-2100, which is a weak PPARγ activator, exhibits potent antidiabetic effects and induces uncoupling protein 1 in white adipose tissue of KKAy obese mice. *Diabetes* **2000**, *49*, 759–767.

(21) Hamza, M. S.; Pott, S.; Vega, V. B.; Thomsen, J. S.; Kandhadayar, G. S.; Ng, P. W.; Chiu, K. P.; Pettersson, S.; Wei, C. L.; Ruan, Y.; Liu, E. T. *De-novo* identification of PPARγ/RXR binding sites and direct targets during adipogenesis. *PLoS One* **2009**, *4*, e4907.

(22) Smallridge, R. C.; Copland, J. A.; Brose, M. S.; Wadsworth, J. T.; Houvras, Y.; Menefee, M. E.; Bible, K. C.; Shah, M. H.; Gramza, A. W.; Klopper, J. P.; Marlow, L. A.; Heckman, M. G.; Von Roemeling, R.

efatutazone, an oral PPAR-γ agonist, in combination with paclitaxel in anaplastic thyroid cancer: results of a multicenter phase 1 trial. *J. Clin. Endocrinol Metab.* **2013**, *98*, 2392–2400.

(23) Serizawa, M.; Murakami, H.; Watanabe, M.; Takahashi, T.; Yamamoto, N.; Koh, Y. Peroxisome proliferator-activated receptor c agonist efatutazone impairs transforming growth factor β2-induced motility of epidermal growth factor receptor tyrosine kinase inhibitor-resistant lung cancer cells. *Cancer Sci.* **2014**, *105*, 683–689.

(24) Choi, J. H.; Banks, A. S.; Kamenecka, T. M.; Busby, S. A.; Chalmers, M. J.; Kumar, N.; Kuruvilla, D. S.; Shin, Y.; He, Y.; Bruning, J. B.; Marciano, D. P.; Cameron, M. D.; Laznik, D.; Jurczak, M. J.; Schürer, S. C.; Vidović, D.; Shulman, G. I.; Spiegelman, B. M.; Griffin, P. R. Antidiabetic actions of a non-agonist PPARgamma ligand blocking Cdk5-mediated phosphorylation. *Nature* **2011**, *477*, 477–481.

(25) Compound **1** was isolated by chiral HPLC (CHIRALPAK AD column, 30 °C column temperature, 4.0 mL/min flow rate, photodiode array detection (254 nm), and mobile phase ethanol/hexane/trifluoroacetic acid=20/80/0.1, 50 mg isopropanol solution injection). Retention time of **1** is 6.5 min and that of the enantiomer of **1** is 5.1 min.

(26) Nolte, R. T.; Wisely, G. B.; Westin, S.; Cobb, J. E.; Lambert, M. H.; Kurokawa, R.; Rosenfeldk, M. G.; Willson, T. M.; Glass, C. K.; Milburn, M. V. Ligand binding and co-activator assembly of the peroxisome proliferator-activated receptor-γ. *Nature* **1998**, *395*, 137–143.

(27) Sheu, S. H.; Kaya, T.;Waxman, D. J.; Vajda, S. Exploring the binding site structure of the PPARγ ligand-binding domain by computational solvent mapping. *Biochemistry* **2005**, *44*, 1193–1209.

(28) Casarotto, M. G.; Craik, D. J. Ring flexibility within tricyclic antidepressant drugs. *J. Pharm. Sci.* **2001**, *90*, 713–721.

(29) Kaminski, J. J.; Carruthers, N. I.; Wong, S. C.; Chan, T. M.; Billah, M. M.; Tozzi, S.; McPhail, A. T. Conformational considerations in the design of dual antagonists of platelet-activating factor (PAF) and histamine. *Bioorg. Med. Chem.* **1999**, *7*, 1413–1423.

(30) Munro, S. L.; Andrews, P. R.; Craik, D. J.; Gale, D. J. ^{13}C NMR studies of the molecular flexibility of antidepressants. *J. Pharm. Sci.* **1986**, *75*, 133–141.

(31) The calculated potential energies of stabel conformations *down-syn* and *up-anti* for (*R*)-1' are 55.906, 54.987 kJ/mol, respectively, and *down-anti* and *up-syn* for (*S*)-1' are 55.907 and 54.987 kJ/mol, respectively. The potential energies of relatively unstable conformations *down-anti* and *up-syn* for (*R*)-1' are 58.839 and 59.100 kJ/mol, respectively, and *down-syn* and *up-anti* for (*S*)-1' were 59.099 and 58.840 kJ/mol, respectively).

(32) Shuto, S.; Ono, S.; Hase, Y.; Kamiyama, N.; Takada, H.; Yamashita, K.; Matsuda, A. Conformational restriction by repulsion between adjacent substituents on a cyclopropane ring: Design and enantioselective synthesis of 1-phenyl-2-(1-aminoalkyl)cyclopropane-*N,N*-diethylcarboxamides as potent NMDA receptor antagonists. *J. Org. Chem*. **1996**, *61*, 915–923.

(33) Shuto, S.; Ono, S.; Hase, Y.; Ueno, Y.; Noguchi, T.; Yoshii, K.; Matsuda, A. Synthesis and biological activity of conformationally restricted analogs of milnacipran: (1*S*,1*R*)-1-Phenyl-2-[(*S*)-1-aminopropyl]-*N,N*-diethylcyclopropanecarboxamide, an efficient noncompetitive *N*-methyl-D-aspartic acid receptor antagonist. *J. Med. Chem*. **1996**, 39, 4844–4852.

(34) Ohmori, Y.; Yamashita, A.; Tsujita, R.; Yamamoto, T.; Taniuchi, K.; Matsuda, A.; Shuto, S. A method for designing conformationally restricted analogues based on allylic strain: Synthesis of a novel class of noncompetitive NMDA receptor antagonists having the acrylamide structure. *J. Med. Chem*. **2003**, *46*, 5326–5333.

(35) Watanabe, M.; Hirokawa, T.; Kobayashi, T.; Yoshida, A.; Ito, Y.; Yamada, S.; Orimoto, N.; Yamasaki, Y.; Arisawa, M.; Shuto, S. Investigation of the bioactive conformation of histamine H_3 receptor antagonists by the cyclopropylic strain-based conformational restriction strategy. *J. Med. Chem*. **2010**, *53*, 3585–3593.

(36) Mizuno, A.; Miura, S.; Watanabe, M.; Ito, Y.; Yamada, S.; Odagami, T.; Kogami, Y.; Arisawa, M.; Shuto, S. Three-dimensional structural diversity-oriented peptidomimetics based on the cyclopropylic strain. *Org. Lett.* **2013**, *15,* 1686–1689.

(37) Kawamura, S.; Unno, Y.; Tanaka, M.; Sasaki, T.; Yamano, A.; Hirokawa, T.; Kameda, T.; Asai, A.; Arisawa, M.; Shuto, S. Investigation of the non-covalent binding mode of covalent proteasome inhibitors

around the transition state by combined use of cyclopropylic strain-based conformational restriction and computational modeling. *J. Med. Chem.* **2013**, *56*, 5829–5842.

(38) Matsui, K.; Kido, Y.; Watari, R.; Kashima, Y.; Yoshida, Y.; Shuto, S. Highly conformationally-restricted cyclopropane tethers with three-dimensional structural diversity drastically enhance the cell-permeability of cyclic peptides. *Chem. Eur. J.* **2017**, *23*, 3034–3041.

(39) Mizuno, A.; Kameda, T.; Kuwahara, T.; Endoh, H.; Ito, Y.; Yamada, S.; Hasegawa, K.; Yamano, A.; Watanabe, M.; Arisawa, M.; Shuto, S. Cyclopropane-based peptidomimetics mimicking wide-ranging secondary structures of peptides: conformational analysis and their use in rational ligand optimization. *Chem. Eur. J.* **2017**, *23*, 3159–3168.

(40) Mizuno, A.; Matsui, K.; Shuto, S. Peptides to peptidomimetics: a strategy based on the structural features of cyclopropane. *Chem. Eur. J.* **2017**,*23*, 14394–14409.

(41) Higgins, L. S.; Mantzoros, C. S. The Development of INT131 as a selective PPARγ modulator: approach to a safer insulin sensitizer. *PPAR Res.* **2008**, Article ID 936906.

(42) Dunn, F. L.; Higgins, L. S.; Fredrickson, J.; DePaoli, A. M. Selective modulation of PPARγ activity can lower plasma glucose without typical thiazolidinedione side-effects in patients with Type 2 diabetes. *J. Diabetes Complications* **2011**, *25*, 151–158.

(43) DePaoli, A. M.; Higgins, L. S.; Henry, R. R.; Mantzoros, C.; Dunn, F. L. Can a selective PPARγ modulator improve glycemic control in patients with type 2 diabetes with fewer side effects compared with pioglitazone? *Diabetes Care* **2014**, *37*, 1918–1923.

(44) NMR spectra of tricyclic compounds at variable temperatures was measured. Consequently, geminal couplings were observed in the signals of the individual benzylic protons in the central seven membered ring of compound **4** and **5** at room temperature (296 K). These data suggest that the two germinal benzylic protons were under different situation where the tricyclic structures are stable in a conformation in solution due to slow flipping of tricyclic scaffold. These results are in accord with the results of NMR conformational analysis of antidepressants with similar 6/7/6-tricyclicstructure (Casarotto, M. G. Craik, D. J. *J. Pharm. Sci.*, **2001**, *90*, 713-721). As the temperature is increased, the peaks of the benzylic protons broaden and then coalesced at 393

K in each compound. Thus, at higher temperature, the conformational flip of the seven-membered ring very rapidly occurs.

(45) Taygerly, J. P.; McGee, L. R.; Rubenstein, S. M.; Houze, J. B.; Cushing, T. D.; Li, Y.; Motani, A.; Chen, J. L.; Frankmoelle, W. ; Ye, G. ; Learned, M. R.; Jaen, J.; Miao, S.; Timmermans, P. B.; Thoolen, M.; Kearney, P.; Flygare, J.; Beckmann, H.; Weiszmann, J.; Lindstrom, M.; Walker, N.; Liu, J,; Biermann, D.; Wanga, Z.; Hagiwara, A.; Iida, T.; Aramaki, H.; Kitao, Y.; Shinkai, H.; Furukawa, N.; Nishiu, J.; Nakamura, M. Discovery of INT131: A selective PPARγ modulator that enhances insulin sensitivity. *Bioorg. Med. Chem.* **2013**, *21*, 979–992.

(46) Takaishi, S.; Okumura, T.; Tu, S.; Wang, S. S.; Shibata, W.; Vigneshwaran, R.; Gordon, S. A.; Shimada, Y.; Wang, T. C. Identification of gastric cancer stem cells using the cell surface marker CD44. *Stem Cells* **2009**, *27*, 1006–1020.

(47) Lundholt, B. K.; Linde, V.; Loechel, F.; Pedersen, H.-C.; Møller, S.; Præstegaard, M.; Mikkelsen, I.; Scudder, K.; Bjørn, S. P.; Heide, M.; Arkhammar, P. O.; Terry, R.; Nielsen, S. J. Identification of Akt pathway inhibitors using redistribution screening on the FLIPR and the IN Cell 3000 Analyzer. *J. Biomol. Screen.* **2005**, *10*, 20–29.

(48) Xu, A.; Lam, M. C.; Chan, K. W.; Wang, Y.; Zhang, J.; Hoo, R. L. C.; Xu, J. Y.; Chen, B.; Chow, W. S.; Tso, A. W. K.; Lam, K. S. Angiopoietin-like protein 4 decreases blood glucose and improves glucose tolerance but induces hyperlipidemia and hepatic steatosis in mice. *Proc. Natl. Acad. Sci. U.S.A.* **2005**, *102*, 6086–6091.

(49) Brasaemle, D. L.; Barber, T.; Wolins, N. E.; Serrero, G.; Blanchette-Mackie, E. J.; Londos, C. Adipose differentiation- related protein is an ubiquitously expressed lipid storage droplet-associated protein. *J. Lipid Res.* **1997**, *38*, 2249–2263.

(50) Kalluri, R.; Neilson, E. G. Epithelial-mesenchymal transition and its implications for fibrosis. *J. Clin. Invest.* **2003**, *112*, 1776–1784.

(51) Einstein, M.; Akiyama, T. E.; Castriota, G. A.; Wang, C. F.; McKeever, B.; Mosley, R. T.; Becker, J. W.; Moller, D. E.; Meinke, P. T.; Wood, H. B.; Berger, J. P. The differential interactions of peroxisome

proliferator-activated receptor γ ligands with Tyr473 is a physical basis for their unique biological activities. J. P. *Mol. Pharmacol.* **2008**, *73*, 62–74.

(52) Hughes, T. S.; Giri, P. K.; de Vera, I. M.; Marciano, D. P.; Kuruvilla, D. S.; Shin, Y.; Blayo, A. L.; Kamenecka, T. M.; Burris, T. P.; Griffin, P. R.; Kojetin, D. J. An alternate binding site for PPARγ ligands. *Nat.Commun.* **2014**, *5*, 3571.

GROUPED TABLES

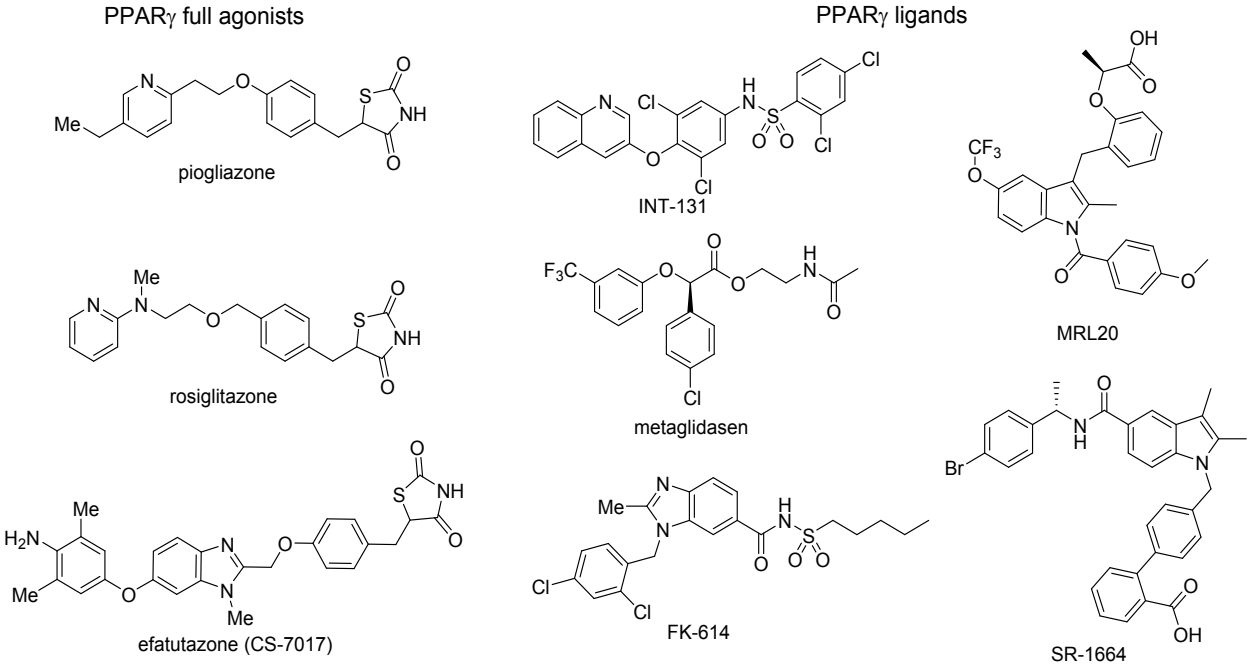

Figure 1. Chemical structures of PPARγ full agonists and ligands.

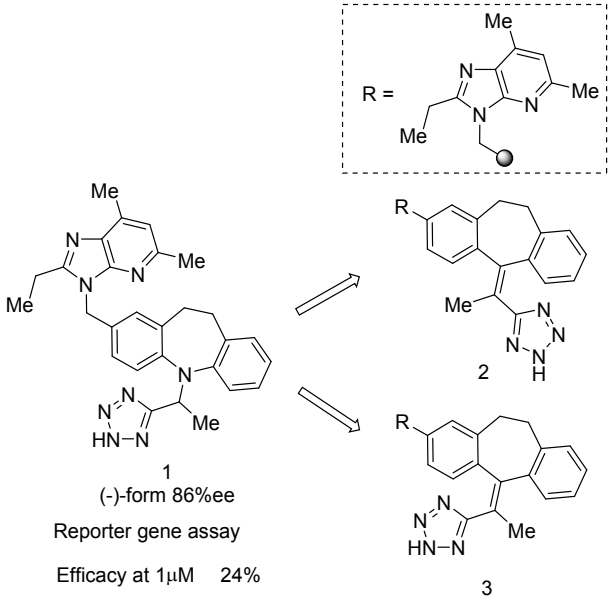

Figure 2. Lead generation approach from screening hit **1**.

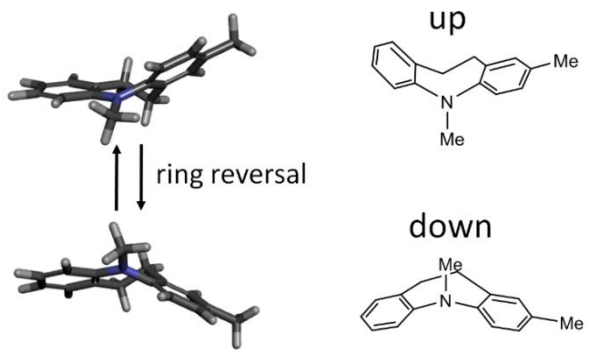

Figure 3. Ring reversal motion of the 6/7/6-tricyclic ring systems.

(A) ***down-syn*** ***up-anti*** (B) ***up-syn*** ***down-anti***

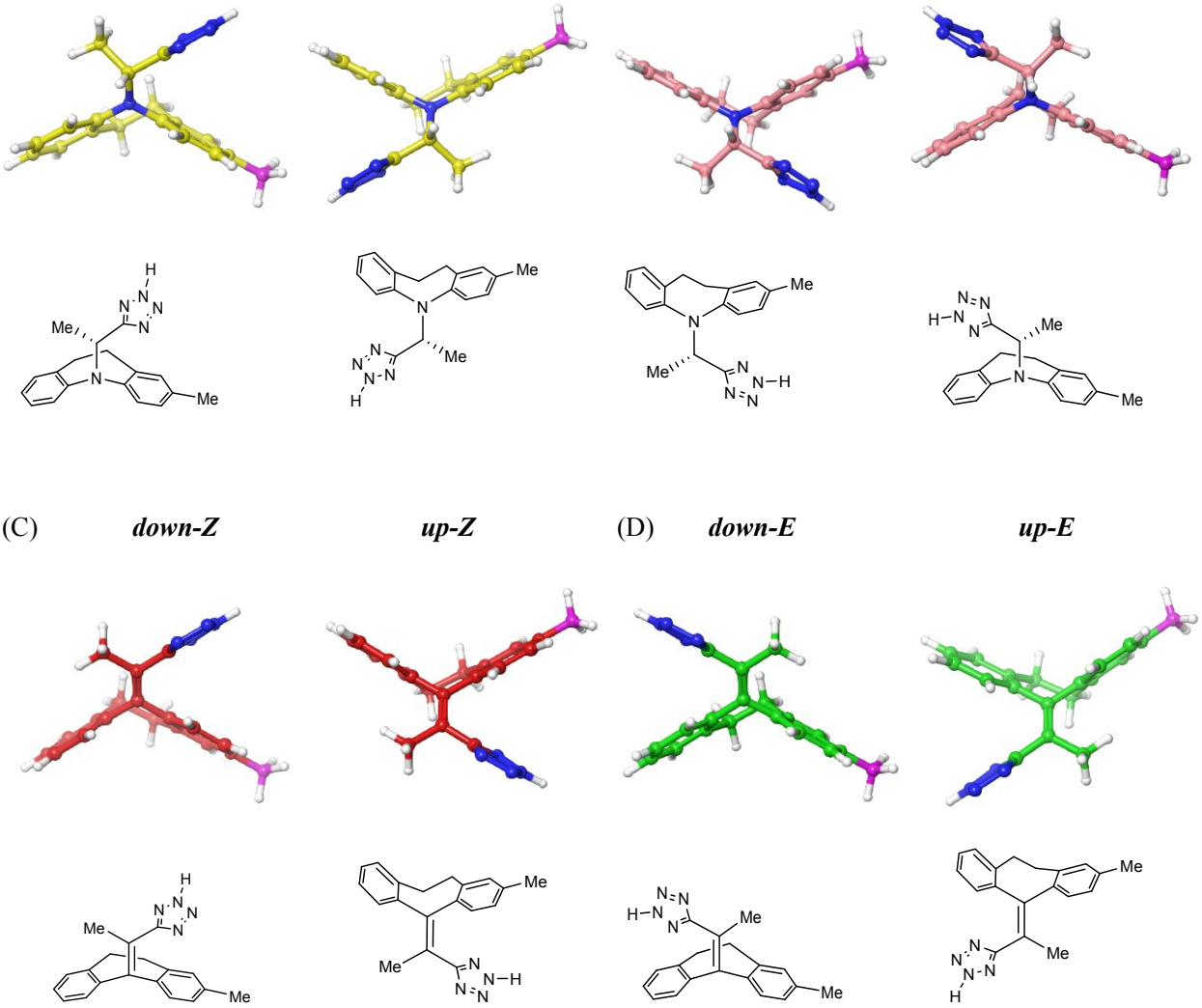

Figure 4. Global energy minimum conformations of (A) (*R*)-**1'** (yellow), (B) (*S*)-**1'** (pink), (C) **2'** (red), (D) **3'** (green) as calculated by the MacroModel. The hydrogens, nitrogens, and 2-methyl group are colored white, blue and magenta respectively.

(A) ***down-syn*** ((*R*)-**1'**) /***down-Z*** (**2'**)

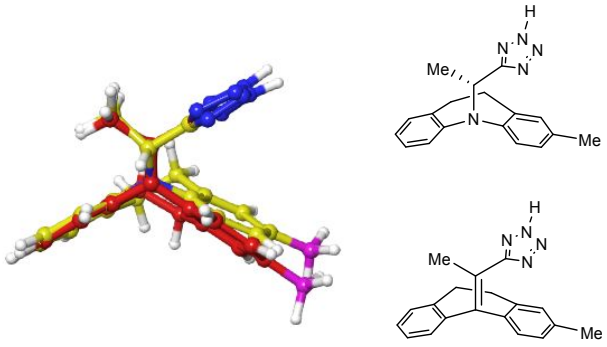

(B) ***up-anti*** ((*R*)-**1'**) /***up-E*** (**3'**)

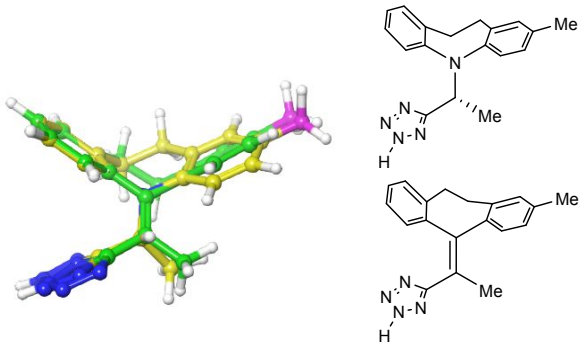

(C) ***up-syn*** ((*S*)-**1'**) /***up-Z*** (**2'**)

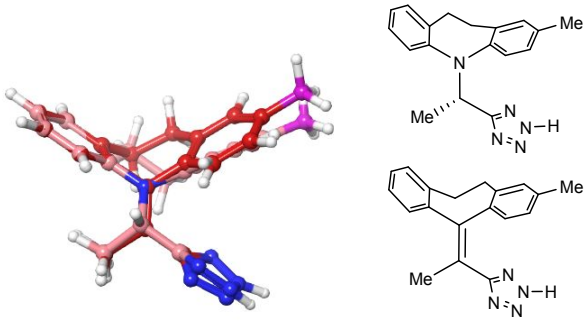

(D) ***down-anti*** ((*S*)-**1'**) /***down-E*** (**3'**)

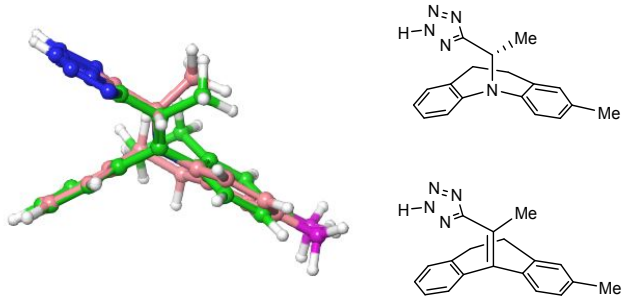

Figure 5. Superimposition of the most stable conformations between compound (*R*)-**1c** (yellow), (*S*)-**1c** (pink), **2c** (red) and **3c** (green) as calculated by the MacroModel. The hydrogens, nitrogens and 2-methyl group are colored white, blue and magenta respectively.

Table 1. PPARγ reporter activities of *E/Z* isomers of dihydrodibenzocycloheptene

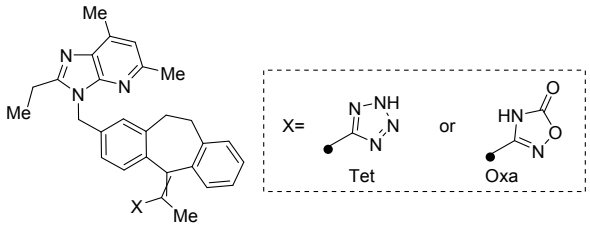

Compd.	Geometric isomer	X	efficacy % at 1 μM	EC_{50} (nM)
1	-	Tet	24	197
2	E	Tet	0.4	-
4	E	Oxa	1.5	-
3	Z	Tet	59	251
5	Z	Oxa	23	177
pioglitazone			100	2053

INT-131	8.3	59
metaglidasen	11	7365

The efficacies and EC_{50} values of compounds **1-5** in human PPARγ /GAL4 transfected HEK293EBNA cells at 24 h after drug treatment. The efficacy of each compound was calculated as the percentage of the maximum activation obtained with pioglitazone at 1000 nM. EC_{50} values were determined using the XLFit.

Table 2. in vitro activities of dihydrodibenzocycloheptene and dibenzo[b,e]oxepine derivatives in PPARγ reporter gene assay

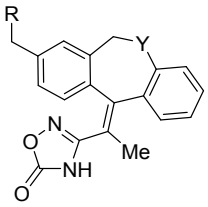

Compd.	R	Y	Reporter gene assay	
			EC_{50} (nM)	Efficacy (%)
5	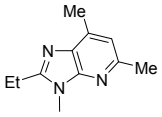	CH_2	177	24
6	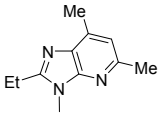	O	84	19
7	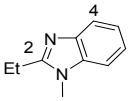	O	17	9.7
8	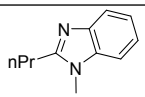	O	2.7	14

9	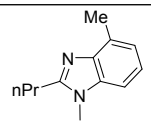	O	2.4	9.5
10	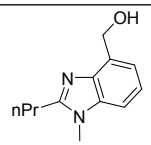	O	33	9.1
11	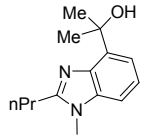	O	13	4.8
12	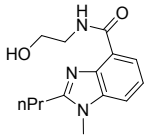	O	57	11
13	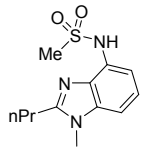	O	166	7.0
14	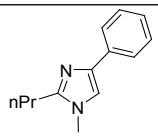	O	151	13
15	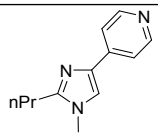	O	593	7.2
pioglitazone			2053	100
INT-131			59	8.3
metaglidasen			7365	11
FK-614			163	11

The efficacies and EC_{50} values of compounds **5-15**, other PPARγ agonists in human PPARγ/GAL4 transfected HEK293EBNA cells at 24h after drug treatment. The efficacy of each compound was calculated as the percentage of the maximum activation obtained with pioglitazone at 1000 nM. EC_{50} values were determined

using the XLFit.

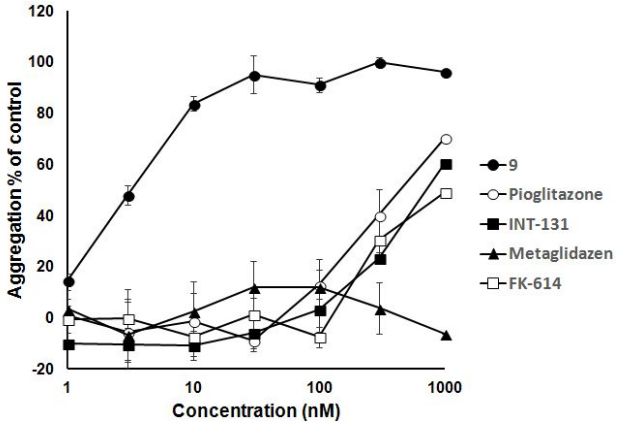

Figure 6. Aggregation activities of PPARγ ligands in MKN-45 cells. The aggregation of MKN-45 cells was evaluated using an IN Cell Analyzer 1000 (GE Healthcare) after treatment of compounds for 5 days. The efficacy of **9** was calculated using its ratio of cell-aggregated clusters as the control value. The aggregation % values of other PPARγ ligands (pioglitazone, INT-131, metaglidasen, FK-614) are shown as the values relative to the maximum efficacy of **9**.

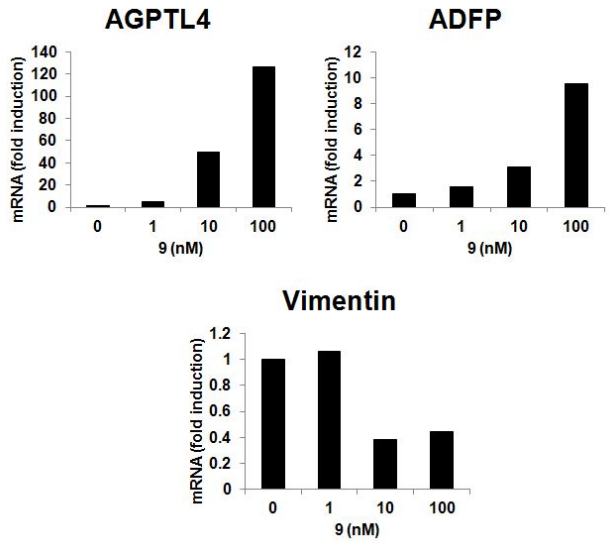

Figure 7. The gene expression in MKN-45 cells after the treatment of **9** at 1-100 nM. The gene expression was determined by quantitative PCR using an ABI PCR system. The fold-inductions are shown as the values relative to baseline.

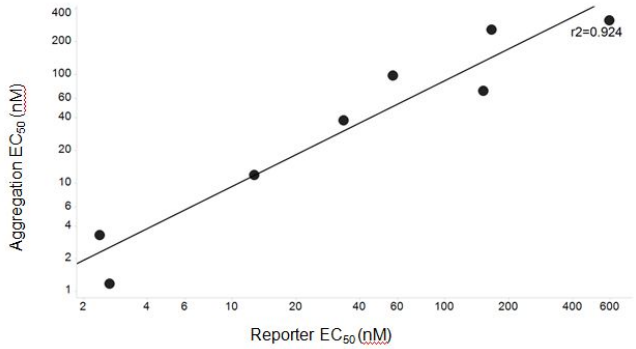

Figure 8. The correlation of the EC_{50} values of tricyclic compounds **8-15** on the aggregation of MKN-45 cells with those obtained in a reporter gene assay for HEK293 cells. There was a strong correlation between the two assays.

(A)

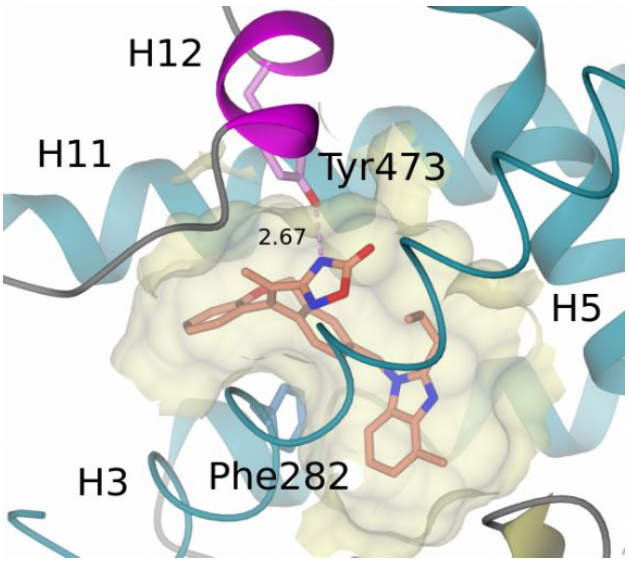

(B)

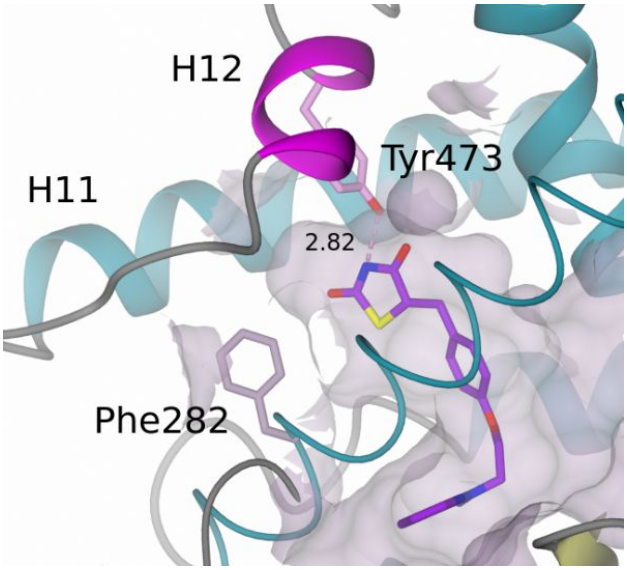

(C)

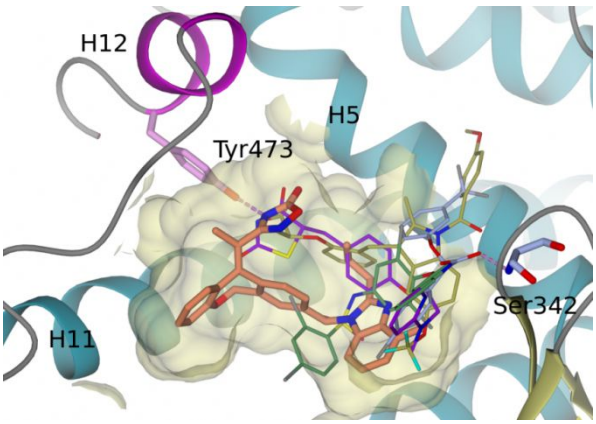

Figure 9. The crystal structures of PPARγ agonists in the PPARγ LBD. (A) The binding mode of **9** (orange) to the PPARγ LBD. The proton of the oxadiazolone ring of **9** interacted with the oxygen atom of Tyr473. (B) The binding mode of rosiglitazone to the PPARγ LBD. Rosiglitazone bound to the canonical site. (C) The overlay of the complex structure of **9**, rosiglitazone (purple, PDB:1FM6), INT-131 (deepgreen, PDB:3FUR), metaglidasen (lightblue, PDB:4PVU), and MRL20 (gold, PDB:2Q59). The acidic group of the ligands interacted with Tyr473.

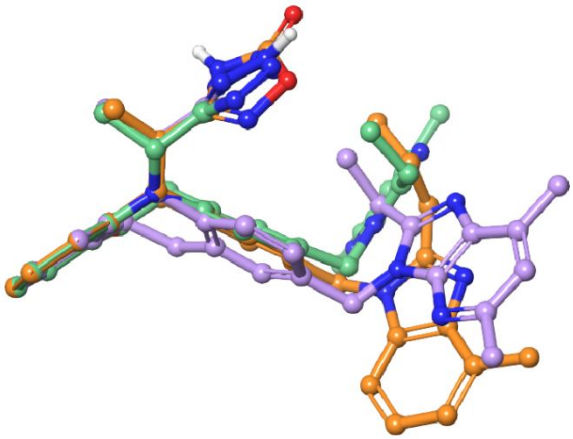

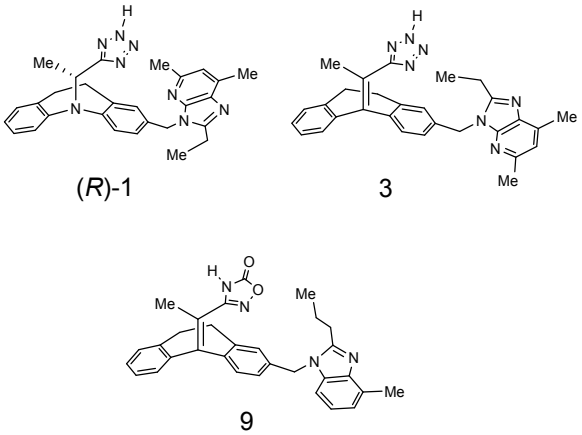

Figure 10. The overlay of the stable conformations *down-syn* of (*R*)-**1** (aquamarine), and *down-Z* of **3** (bluepurple) as calculated by the MacroModel and the structure of **9** (orange) from the crystal structure with the PPARγ LBD.

Scheme 1. Synthesis of dihydrodibenzocycloheptene and dibenzooxepine compounds [a]

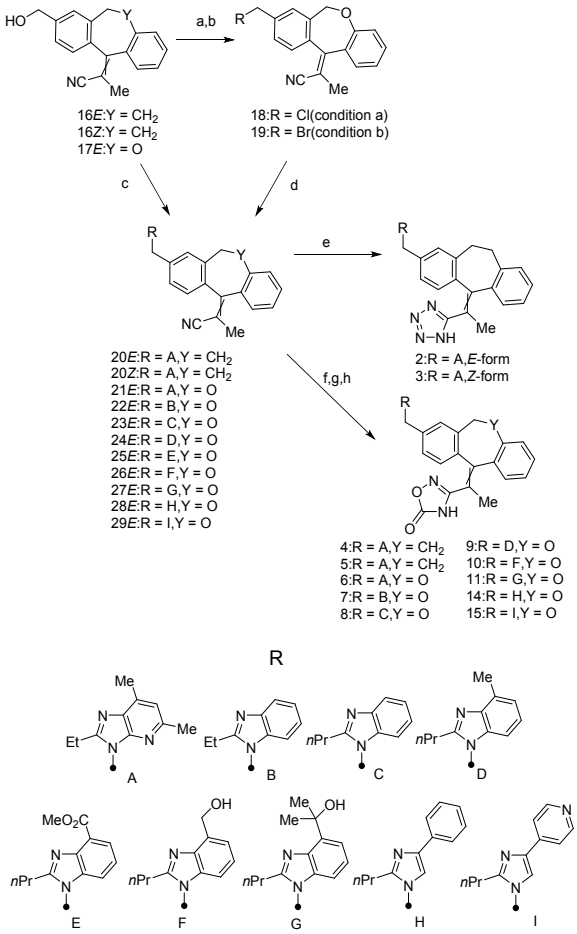

[a]Reagents: a) MsCl, LiCl, Et_3N, THF; b) Ms_2O, LiBr, 2,6-lutidine, THF; c) RH, DTBAD, ps-PPh_2, THF; d) RH, K_2CO_3, DMF; e) $TMSN_3$, nBu_2SnO, toluene, 90 °C; f) 50% H_2NOH aq., EtOH, reflux; g) $ClCO_2Et$, pyridine or Et_3N, CH_2Cl_2; h) *tert*-BuOK, toluene, THF.

Scheme 2 Modification of the substituents in 4-position on benzoimidazole ring [a]

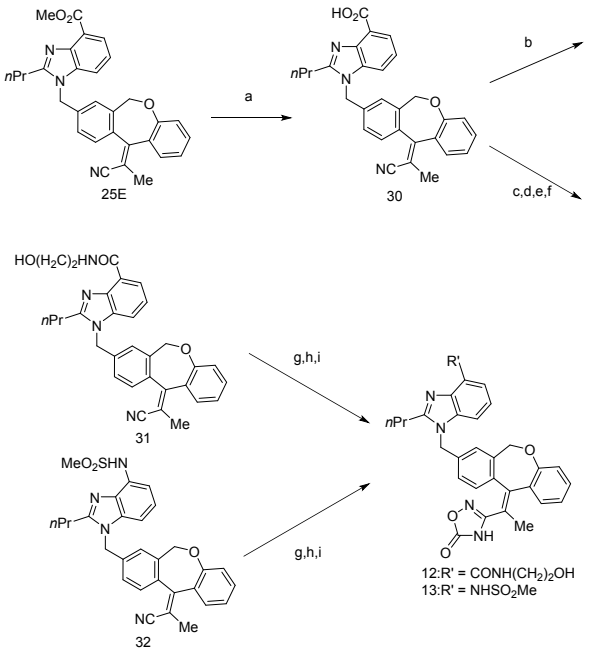

[a]Reagents: a) 4M NaOH, EtOH, 60 °C; b) $NH_2(CH_2)_2OH$, EDCI·HCl, HOBt, DMF; c) DPPA, Et_3N, $CHCl_3$; d) *t*BuOH, reflux; e) TFA, CH_2Cl_2; f) $MeSO_2Cl$, DMAP, pyridine; g) 50% H_2NOH aq., EtOH, reflux; h) $ClCO_2Et$, pyridine or Et_3N, CH_2Cl_2; i) *tert*-BuOK, toluene, THF.

TABLE OF CONTENTS GRAPHIC

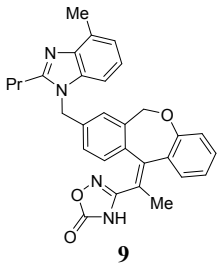

9

Reporter gene assay EC_{50}
2.4 nM

MKN-45 differentiation
94% at 30 nM

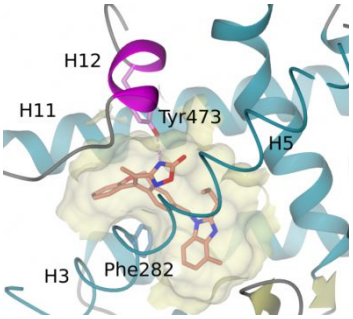

Unique binding mode to PPARγ-LBD